Sources and lesion-induced changes of VEGF expression in brainstem motoneurons

Silvia Silva-Hucha, Génova Carrero-Rojas, María Estrella Fernández de Sevilla, Beatriz Benítez-Temiño, María América Davis-López de Carrizosa, Angel M Pastor, Sara Morcuende*

Departamento de Fisiología, Facultad de Biología,

Universidad de Sevilla, Sevilla, Spain

Correspondence:

Dr. Sara Morcuende

e-mail: smorcuende@us.es

Tel: +0034 954559549

ORCID S.S.H. 0000-0002-8026-502X

ORCID G.C.R. 0000-0002-1984-3505

ORCID M.E.F.D.S. 0000-0002-2693-1861

ORCID B.B.T. 0000-0002-3852-1093

ORCID M.A.D.L.D.C. 0000-0002-2551-3115

ORCID A.M.P. 0000-0002-6213-7454

ORCID S.M. 0000-0003-1471-7005

Abstract

Motoneurons of the oculomotor system show lesser vulnerability to neurodegeneration compared to other cranial motoneurons, as seen in amyotrophic lateral sclerosis (ALS). Overexpression of vascular endothelial growth factor (VEGF) is involved in motoneuronal protection. As previously shown, motoneurons innervating extraocular muscles present a higher amount of VEGF and its receptor Flk-1 compared to facial or hypoglossal motoneurons. Therefore, we aimed to study the possible sources of VEGF to brainstem motoneurons, such as glial cells and target muscles. We also studied the regulation of VEGF in response to axotomy in ocular, facial and hypoglossal motor nuclei.

Basal VEGF expression in astrocytes and microglial cells of the cranial motor nuclei was low. Although the presence of VEGF in the different target muscles for brainstem motoneurons was similar, the presynaptic element of the ocular neuromuscular junction showed higher amounts of Flk-1, which could result in greater efficiency in the capture of the factor by oculomotor neurons.

Seven days after axotomy, a clear glial reaction was observed in all the brainstem nuclei, but levels of the neurotrophic factor remained low in glial cells. Only the injured motoneurons of the oculomotor system showed an increase in VEGF and Flk-1, such an increase was not detected in axotomized facial or hypoglossal motoneurons. Taken together, our findings suggest that the ocular motoneurons themselves upregulates VEGF expression in response to lesion.

In conclusion, the low VEGF expression observed in glial cells suggests that these cells are not the main source of VEGF for brainstem motoneurons. Therefore, the higher VEGF expression observed in motoneurons innervating extraocular muscles is likely due either to the fact that this factor is more avidly taken up from the target muscles, in basal conditions, or is produced by these motoneurons themselves, and acts in an autocrine manner after axotomy.

Keywords: oculomotor system, VEGF, Flk-1, brainstem motoneurons, axotomy, amyotrophic lateral sclerosis.

Acknowledgments

Confocal microscopy imaging was performed in the central research services of the Universidad de Sevilla (CITIUS). This work was supported by the Ministerio de Economía y Competitividad (Grant reference: BFU2015-64515-P and PGC2018-094654-B-100), and Consejería de Economía, Innovación, Ciencia y Empleo, Junta de Andalucía, BIO-297, in Spain. Confocal images were performed in the Central Research Services of University of Sevilla (CITIUS). We acknowledge Dr. Paul J May from UMMC for helpful comments and editing the manuscript.

Author contributions

S.M., S.S.H., A.M.P., M.A.D.L.C. and B.B.T. designed experiments. S.M., S.S.H., B.B.T., G.C.R., M.E.F.S. and A.M.P. performed experiments. S.M., S.S.H., B.B.T. analyzed and processed the data. S.M. wrote the manuscript. S.M., A.M.P., M.A.D.L.C. and B.B.T. proofread and edited the manuscript. All authors read and approved the final version of the manuscript.

Compliance with ethical standards

This study was carried out in accordance with the recommendations of the University of Seville ethics committee

Conflict of interest statement

The authors declare no conflict of interest.

1. Introduction

Brainstem motoneurons are differentially affected by degeneration, induced either by nerve insults or by neurodegenerative diseases, such as amyotrophic lateral sclerosis (ALS) (Reiner et al., 1995; Nimchinsky et al., 2000; Haenggeli and Kato, 2002). Specifically, motoneurons of the oculomotor system, located in the oculomotor (III; OCM), trochlear (IV; TRO) and abducens (VI; ABD) nuclei, have less vulnerability to neurodegeneration compared to other cranial motoneurons, as seen in ALS. Commonly, facial (VII) and hypoglossal (XII; HYPO) motor nuclei are more affected in this disease.

Trophic factors are known to play a principal role in neuronal survival in adult motoneurons, including motoneurons of the oculomotor system (for review see Benítez-Temiño et al., 2016). In recent years, vascular endothelial growth factor (VEGF) has been included in the group of trophic factors acting on motoneurons (Storkebaum et al., 2004; Bogaert et al., 2006; Lange et al., 2016; Calvo et al., 2018b). VEGF was initially discovered as a vascular permeability factor (Senger et al., 1983) and considered an endothelial specific growth factor. However, VEGF´s role in neuroprotection became evident when mice with reduced level of VEGF ($VEGF^{\delta/\delta}$) developed adult-onset progressive motoneuronal degeneration, resembling ALS (Oosthuyse et al., 2001). Recent discoveries prove that VEGF has direct effects on neurons, stimulating axonal outgrowth and survival (Zheng et al., 2004; Storkebaum et al., 2005; Tolosa et al., 2009; Tovar-y-Romo and Tapia, 2012; Lladó et al., 2013; Pronto-Laborinho et al., 2014). Accordingly, VEGF upregulation plays a neuroprotective role in neurons (Lambrechts et al., 2003; Sun et al., 2003; Wang et al., 2007), while blockade of VEGF activity leads to neuronal degeneration (Oosthuyse et al., 2001; Devos et al., 2004; Sathasivam, 2008).

VEGF binds the receptors tyrosine kinase VEGFR-1 (Flt-1) and VEGFR-2 (KDR/Flk-1), but neuronal effects are mainly mediated by the latter (Sondell et al., 2000). Receptor activation leads to PI3K/Akt signaling, inhibiting p38 MAP kinase phosphorylation. This lowered phosphorylation prevents Bcl-2 downregulation and inhibits apoptosis (Li et al., 2003; Tolosa et al., 2009).

The effects of VEGF as a neuroprotective factor on motoneurons innervating extraocular muscles was recently revealed (Acosta et al., 2018; Calvo et al., 2018a). Furthermore, we have previously demonstrated that oculomotor motoneurons show a higher expression of the neurotrophic factor VEGF and its main receptor Flk-1 than other brainstem motoneurons in adult rats (Silva-Hucha et al., 2017). It seems reasonable to propose that since low VEGF levels lead to motoneuronal degeneration, higher VEGF expression in ocular motoneurons could be related their resistance to degeneration.

VEGF has been demonstrated to access motoneurons somata via retrograde transport from the target muscles (Azzouz et al., 2004; Krakora et al., 2013). In addition, VEGF can be produced by the motoneurons themselves (Ogunshola et al., 2002; Murakami et al., 2003; Croll et al., 2004; McCloskey et al., 2008), and may act in an autocrine manner. Another possibility is that VEGF may be supplied to the motoneurons from the surrounding glial cells, in a paracrine way (Ijichi et al., 1995; Krum and Rosenstein, 1998; Zhou et al., 2019). Therefore, we were interested in exploring whether differences exist in the sources of VEGF for brainstem motoneurons, and whether astrocytes, microglial cells and target muscles provide the motoneurons of ocular system higher baseline levels of VEGF than are available to more vulnerable brainstem motoneurons. We examined the possible source of VEGF for motoneurons by means of immunohistochemistry and Western blotting.

One common event that occurs after the induction of a variety of different types of brain insult, such as excitotoxicity, vessels occlusion or seizures, is an increase in VEGF of Flk-1 expression in motoneurons or in glial cells (Lennmyr et al., 1998; Croll et al., 2004; McCloskey et al., 2008; Nicoletti et al., 2008; Castañeda-Cabral et al., 2017). This upregulation has been related to neuroprotection, and avoidance of motoneurons degeneration. Therefore, we were also interested in studying the regulation of VEGF and its receptor on neurons and glial cells of brainstem motor nuclei in response to injury. To this end, we used cranial nerve axotomy, a well characterized injury to brainstem motoneurons that interrupt retrograde transport (Kobayashi et al., 1996; Morcuende et al., 2011), as our injury model. To determine the variations in VEGF expression, we examined control and axotomized nuclei by immunohistochemistry and quantitative PCR (qPCR).

2. Material and methods

2.1. Animals and tissue extraction

Adult Wistar rats were obtained from an authorized supplier (University of Seville). All experimental procedures were performed in accordance with the guidelines of the European Union (2010/63/EU) and Spanish legislation (R.D. 53/2013, BOE 34/11370-421) for the use and care of laboratory animals and were approved by the local committee for animal research. All efforts were made to minimize the number of animals used and their suffering in this study. A total of 44 animals were used in the present work: 18 were control non-operated animals, and 26 were axotomized.

Animals destined to immunohistochemistry were sacrificed by intracardiac perfusion. Under deep anesthesia (sodium pentobarbital, 50 mg/kg, i.p.) animals were perfused with 100 ml of physiological saline, followed by 250 ml of 4 % paraformaldehyde in 0.1 M sodium phosphate buffer, pH 7.4 (PB). The brainstem was removed and cryoprotected by immersion in a solution of 30 % sucrose in sodium phosphate-buffered saline (PBS) until they sink. Tissue was then cut into 40 μm-thick coronal sections using a cryostat (Leica CM1850, Wetzlar, Germany).

In control animals (n = 4), brainstem sections were divided in two series: one for GFAP immunohistochemistry, and the other for Iba1. Alternate sections from each animal were used to perform an analysis of VEGF expression in astrocytes and microglial cells, respectively. Cranial muscles from control animals (n = 8) were processed for immunohistochemistry against VEGF or Flk-1.

Brainstems from axotomized animals (n = 4) were sectioned and separated in two series with the following purposes. The first series served for analysis of possible changes in VEGF expression between different groups of lesioned motoneurons. This was done by double immunocytochemistry against ChAT and VEGF. The other series was processed with double immunohistochemistry against ChAT and Flk-1, to detect changes in the expression of the receptor after axotomy. Brainstems from a second set of axotomized animals (n = 4) were sectioned and used in alternating order to stain either for astrocytes or microglia. Antibodies against GFAP or Iba1, plus VEGF and ChAT, were used to study the expression of VEGF in these glial cells after lesion.

Animals destined to Western blot (n = 6) or qPCR (n = 18) techniques were sacrificed under deep anesthesia (sodium pentobarbital, 50 mg/kg, i.p.), then the tissue was extracted and immediately frozen.

2.2. Surgical procedure: axotomy

Animals prepared for axotomy were operated on under general anesthesia (sodium pentobarbital, 35 mg/kg, i.p.). Axotomy of the oculomotor, facial and hypoglossal nerves was performed in different groups of adult rats. Surgery consisted in the enucleation of the left eye, as a method to axotomize motoneurons innervating extraocular muscles, or the ligation and cutting of the left facial or left hypoglossal nerve, leaving the corresponding motoneurons deprived from their target muscles. The procedure for enucleation has been described in detail previously (Morcuende et al., 2005, 2011, 2013). Briefly, the left eyeball was extirpated, intraorbital tissues removed and bleeding cauterized. Eyelids were then sutured closed over the orbit. Animals were sacrificed 7 days after axotomy, since that survival time was found to be the optimum for detecting changes in neurotrophic factor expression in previous studies (Navarro et al., 2007; Morcuende et al., 2011). As indicated above, tissue from axotomized animals was treated according to the technique: immunohistochemistry or qPCR.

2.3. Immunohistochemistry

2.3.1. Immunohistochemistry in brain tissue

To determine VEGF expression in motoneurons, astrocytes and microglial cells, in control or lesioned brainstem nuclei, double or triple confocal immunohistochemistry was performed. The following antibodies were used as markers of specific populations of brains cells: choline acetyl-transferase (ChAT) as a marker for motoneurons, glial fibrillary acidic protein (GFAP) as a marker for astrocytes, and Iba1 as a marker for microglial cells. Triple immunofluorescences were made using ChAT along with VEGF antibodies, and used another marker for glial cells, either GFAP or Iba1, to characterize, on one hand, the

presence of VEGF on glial cells, and on the other hand, possible differences in the expression of this protein in response to lesion. Double immunohistochemistry, using ChAT along with either VEGF or Flk-1 antibodies, was used to visualize possible changes in VEGF of Flk-1 expression in axotomized motoneurons. Rhodamine (TRICT), fluorescein (FITC) and cyanine-5 (Cy5) were used as fluorophores coupled to the secondary antibodies.

For double ChAT-VEGF immunohistochemistry, nonspecific binding was blocked by incubation for 45 minutes in a solution consisting of 10 % normal donkey serum in PBS with 0.01 % Triton X-100 (PBS-T). Sections were then incubated overnight at room temperature with the primary antibody solution containing goat polyclonal anti-ChAT IgG from Millipore (Billerica, MA, USA; AB-144P, 1:500) and rabbit polyclonal anti-VEGF IgG (Santa Cruz Biotechnology, Dallas, TX, USA; sc-507, 1:200) prepared in PBS-T with 5 % of normal donkey serum. After several rinses in PBS-T, sections were incubated for 2 hours in a solution with the secondary antibodies diluted in PBS-T: donkey anti-goat-TRITC IgG (Jackson ImmunoResearch, West Grove, PA, USA; 705-025-003, 1:100) and donkey anti-rabbit-FITC IgG (Jackson ImmunoResearch; 711-095-152, 1:50).

In alternate sections from the same animal, double immunohistochemistry against ChAT and Flk-1 was performed. After blocking the non-specific binding, sections were incubated overnight at room temperature with goat polyclonal anti-ChAT IgG from Millipore (AB-144P, 1:500). The antibody binding was visualized by incubating tissue with an anti-goat-TRITC IgG (Jackson ImmunoResearch; 705-025-003, 1:50). Then, sections underwent incubation with mouse monoclonal anti-Flk-1 IgG (Santa Cruz Biotechnology; sc-6251, 1:500) prepared in PBS-T with 5 % of normal donkey serum overnight. After several rinses in PBS-T, sections were incubated for 2 hours in the secondary antibody solution (donkey anti-mouse-FITC IgG; Jackson ImmunoResearch; 715-095-150, 1:50).

For triple ChAT-VEGF-GFAP immunohistochemistry, the double protocol described above was followed, and afterwards, sections were rinsed in PBS-T and incubated overnight in a monoclonal antibody against GFAP (mouse anti-GFAP, Sigma-Aldrich, St. Louis, MO, USA; G3893, 1:300), followed by a secondary donkey Cy-5 anti-mouse (Jackson ImmunoResearch; 715-175-150, 1:100).

For triple ChAT-VEGF-Iba1 immunohistochemistry, a similar protocol as above was performed, but a mouse monoclonal anti-VEGF was used instead (Abcam, Cambridge, MA, USA; ab1316, 1:500), with a secondary anti-mouse coupled to FITC (Jackson ImmunoResearch; 715-095-150, 1:200). Microglial cells were labelled by using a polyclonal rabbit antibody anti-Iba1 (Wako; 019-19741, 1:1000), followed by incubation in donkey anti-rabbit Cy5 (Jackson ImmunoResearch; 711-175-152, 1:100)

Sections were then washed several times, mounted on gelatinized glass slides and coverslipped with fluorescent mounting medium (DAKO, Glostrup, Denmark; S3023). Confocal microscopy images were captured at 40X magnification with a confocal laser-scanning microscope (Zeiss LSM 7 DUO, Oberkochen, Germany), and were later analyzed by using the program Image J (NIH, Bethesda, MD, USA).

To quantify the percentage of astrocytes and microglial cells which expressed VEGF in control conditions, mean gray value (optical density) inside the cell body and processes was measured. For background correction, five optical density readings of similar area to glial cells were taken per image in areas devoid of motoneurons. Then, the optical density value of every cell was divided by the mean background level determined for the same image. Glial cells were considered positive for VEGF when they showed an optical density value at least three times higher than the background level (Silva-Hucha et al., 2017).

In axotomized animals, due to the large glial reaction, a different technique was used to quantify VEGF expression by the glial cells. Optical density of VEGF, GFAP or Iba1 was measured in both sides, control and injured, using a grid consisting in squares of 10 x 10 μm spaced every 10 μm. Within each square where glial cells were present, we measured the optical density, excluding those containing motoneurons. In the case of motoneurons, VEGF or Flk-1 signal intensity was measured by outlining the soma, avoiding the cell nucleus. Data of lesioned side were expressed as percentage relative to the control side of the same histological section.

2.3.2. Immunohistochemistry in muscle tissue

Immunohistochemistry was also performed to localize and analyze VEGF and its receptor, Flk-1, in the target muscles for the respective cranial nerves.

For VEGF immunohistochemistry, rats were perfused, as described above, and extraocular, buccinator and tongue muscles were dissected and cryoprotected in 30% sucrose for 12 hours. Then, the muscles were frozen in liquid nitrogen and sectioned into 18 µm-thick sections using a cryostat. These were mounted onto gelatinized slides to undergo immunohistochemistry. Triple labelling was performed combining VEGF immunolabelling (mouse anti-VEGF, Abcam; ab1316, 1:500), with phalloidin-Atto 647 N (Sigma-Aldrich; 65906, 1:200), which labels actin filaments, and is used as a marker of muscle fibers, and DAPI (Sigma-Aldrich; D9542, 1:10000), in order to identify the cell nuclei. After confocal capture of images, the VEGF signal was measured inside the muscle fibers.

For Flk-1 immunohistochemistry on muscles, another group of rats were perfused and the muscles extracted. Whole muscles were treated with 4%β-mercaptoethanol and 1% sodium dodecyl sulphate (SDS) in PB for 10 minutes, to unmask antigens. Immunolabelling for Flk-1 (mouse anti-Flk-1 IgG; Santa Cruz Biotechnology; sc-6251, 1:500) was combined with antibody labelling for neurofilaments, to label axons in the muscle (NeuM, rabbit polyclonal, Millipore; AB1987, 1:1000), and α-bungarotoxin tetramethylrhodamine (Sigma-Aldrich; T0195, 1:500), to label the postsynaptic element by binding to the nicotinic acetylcholine receptors. Confocal images of this material were analyzed to delimit the presynaptic element of the neuromuscular junction and quantifying the Flk-1 signal present in it.

2.4. Western blot

Expression of VEGF and Flk-1 in target muscles was also analyzed by Western blotting. Under stereomicroscopic observation, the extraocular muscles, the buccinator and the tongue muscles were dissected. In the case of the tongue, care was taken to remove the mucosa to avoid the presence of salivary glands, which are rich in neurotrophic factors. The tissue was homogenized in cold lysis buffer containing a cocktail of protease and phosphatase inhibitors (Morcuende et al., 2013), disrupted by sonication and centrifuged at 13000 rpm for 30 minutes. The supernatants were isolated and total protein concentrations were determined by the Bradford method, using BSA as a standard. Proteins were diluted in sample buffer and denatured at 95°C for 6 minutes, and then were separated by 15 % (VEGF) or 7.5 % (Flk-1) SDS PAGE (50 µg/lane), before been transferred to PVDF membrane by electroblotting. To reduce nonspecific binding, the membranes were blocked for 1 hour with 10 % BSA, and then blots were incubated overnight at 4°C in a solution containing anti-VEGF rabbit polyclonal antibody (Abcam; ab46154, 1:1000) or anti-Flk-1 rabbit polyclonal antibody (Abcam; ab11939, 1:1000), diluted in TBS-Tween 0.1 % supplied with 5 % BSA. After washing three times with PBS-Tween buffer, the membranes were incubated with horseradish peroxidase-conjugated anti-rabbit antibody (Vector Labs; PI-1000, 1:200) 1 hour at room temperature. The immunoreaction was detected using the WesternBright Quantum kit (Advansta, Menlo Park, CA, USA; K-12042). The chemiluminiscence was visualized using a Luminescent Image Analyzer (LAS-3000, Fuji Photo Film GmbH, Düsseldorf, Germany). After washing the membranes for 10 minutes with stripping buffer, blots were re-probed with anti-glyceraldehyde 3-phosphate dehydrogenase (GAPDH) mouse monoclonal antibody (Millipore; MAB374, 1:1000) to ensure equal loading. The density of the immunoreactive bands was quantified by densitometry using the Multi Gauge software (Fuji Photo Film, Japan). The data were normalized to the GAPDH level for each sample. VEGF or Flk-1 expression in buccinator and tongue muscles was expressed relative to that found in the oculomotor muscles for each Western blot.

2.5. Quantitative PCR

The effect of axotomy on the expression of VEGF and Flk-1 in the oculomotor, facial and hypoglossal nuclei was assessed by qPCR. For this purpose, brains were dissected and 150 µm-thick brainstem sections were obtained using a cryostat. The area occupied by the nuclei of interest in each section was then isolated, with special care to separately collect the control and affected sides. For the motoneurons of the oculomotor system, the oculomotor complex (OCM) was isolated, containing motoneurons of the oculomotor and trochlear nuclei (Haenggeli and Kato, 2002; Silva-Hucha et al., 2017). Tissue was placed in an Eppendorf containing RNAprotect Cell Reagent (Qiagen, USA), and a mechanical dissociation was performed using a p1000, and then a p100 micropipette. Total mRNA was then extracted following the protocol of the RNAeasy Plus Micro kit (Qiagen), and cDNA was synthesized using the QuantiTect Reverse Transcription Kit (Qiagen). The amount of cDNA was measured using a NanoDrop2000 (ThermoFischer Scientific; USA), and samples were stored at 100 ng/µl in water. Specific cDNA of VEGF and Flk-1, as

well as the housekeeping genes actine-b (Act) and phosphoglycerate kinase-1 (PGK-1), were amplified according to the kit guidelines (SensiFAST SYBR; Bioline, UK). Reactions were run in triplicates using LightCycler 480 equipment (Roche Molecular Systems, USA). The qPCR protocol started with a predenaturation step (95 ºC for 2 min) followed by 40 reaction cycles including three sequential periods: denaturation (95 ºC for 5 s), annealing (60 ºC for 13 s) and extension (72 ºC for 7 s). The specificity of the amplification protocol was assessed by a melt curve analysis using LightCycler 480 software. Threshold cycles (Ct) were determined by the second derivative of the fluorescence curve. Relative quantification using ΔΔCt was carried out and data were relativized to EOM results.

Predesigned Act and PGK-1 primers were obtained from PrimePCR Assays and Controls (BioRad, Act: qRnoCID0056984; PGK-1: qRnoCED0002588). VEGF and Flk-1 primers were custom-designed using sequence databases (NCBI, USA) and free software (OligoCalc, Biotools, USA; VEGF Fwd: 5' - TGCACTGGACCCTGGCTTTA - 3'; VEGF Rv: 5' - CACACAGGACGGCTTGAAGA - 3'; NCBI Reference Sequence: AF062644; Flk-1 Fwd: 5' - GTTGGTGGAGCACTTGGGAA - 3'; Flk-1 Rv: 5' - TAGGCAGGGAGAGTCCAGAA - 3', NCBI Reference Sequence: NM_013062.1).

2.6. Statistics

Data were represented as the mean and standard error of the mean (SEM). Western blot data of facial and hypoglossal nuclei are presented as relative measures compared to data obtained in oculomotor nuclei (= 1). Immunohistochemistry and qPCR data of axotomized animals are presented as percentage of expression of VEGF, Flk-1, GFAP or Iba1 in lesioned nuclei with respect to their control sides values (= 100 %).

To detect differences between groups, the one-way ANOVA test was used at an overall level of significance of 0.05 followed by the post hoc Holm-Sidak method for all pairwise multiple comparisons. When required, we also used the paired t-test for comparisons between the nuclei of the control and the axotomized sides. Statistics was performed by using the program SigmaPlot 11 (Systat Software, Inc., Chicago, IL, USA).

3. Results

One of the two main objectives of this work was to study the possible sources of the neurotrophic factor VEGF for motoneurons located in the motor nuclei of the brainstem. For that purpose, we first analyzed VEGF expression in cells which could be contributing this factor through paracrine mechanisms. The glial cells surrounding motoneurons (astrocytes and microglial cells) in the brainstem motor nuclei represent one such source. VEGF could also be reaching the soma of motoneurons through retrograde transport from the target muscles, so the second possibility we explored was the muscle as a possible source of VEGF. Even the motoneurons themselves could produce the trophic factor VEGF and regulate its production. The third possibility we explored was self-production of VEGF by the motoneurons, through the use of qPCR.

For the second main objective, we undertook a series of experiments in which we investigated whether VEGF and Flk-1 receptor could vary their presence in the brainstem nuclei in response to injury. Towards this end, we selectively axotomized the extraocular (III, IV and VI), or the facial (VII), or the hypoglossal nerve (XII) to study the response of axotomized motoneurons and surrounding glial cells with respect to the expression of VEGF and its receptor Flk-1.

3.1. Basal expression of VEGF in astrocytes of brainstem motor nuclei.

Immunohistochemistry was performed on control brainstem tissue to determine the basal VEGF expression by astrocytes of the five motor nuclei. For that purpose, sections that had undergone triple immunohistochemistry using antibodies against ChAT, VEGF and GFAP were analyzed by confocal microscopy.

In normal material, only a small number of GFAP-positive astrocytes were present in oculomotor nuclei, mainly located at the edges of the nuclei, and near the midline (Fig. 1a-b). As can be seen in Fig. 1c, VEGF-labelling was faint in the neuropil surrounding ocular motoneurons. On the other hand, the

motoneuron somata showed intense VEGF-labelling in their cytoplasm. As the results were very similar in each of the three motor nuclei of the ocular system, only images of the oculomotor nucleus are shown in the figures.

The number and distribution of GFAP-labelled astrocytes in facial and hypoglossal nuclei (Fig. 1d-e, g-h, respectively) was similar to that seen in the ocular motor nuclei. In the latter nucleus, greater number of astrocytes was found at the ventricular edge and in the midline. As was the case in the oculomotor nuclei, astrocytes at these two nuclei expressed low levels of VEGF (Fig. 1f and i).

The percentage of VEGF-positive astrocytes was evaluated by quantifying the VEGF optical density within astrocytes in every motor nucleus studied. When the percentage of astrocytes positive for VEGF labelling was compared between oculomotor nuclei (ABD: 32.56 ± 6.52 %; TRO: 18.23 ± 8.69 %; OCM: 19.61 ± 8.13 %) and non-oculomotor nuclei (facial and hypoglossal: 21.20 ± 4.91 % and 36.61 ± 7.85 %, respectively), no significant differences were obtained (one-way ANOVA, $p > 0.05$; $n = 4$; Fig. 1j).

Therefore, these results show that the astrocytes of the motor nuclei located in the brainstem do not exhibit high amounts of VEGF, and show no differences in VEGF expression between them.

3.2. Basal expression of VEGF in microglial cells surrounding brainstem motoneurons.

We also aimed to determine the basal expression of VEGF in the microglial cells present in the brainstem motor nuclei. To this end, an antibody against Iba1 was used as a marker for microglial cells, together with markers for VEGF and ChAT, the latter allowing the identification of the motoneurons and to recognize the motor nuclei.

Iba1-positive microglial cells were observed intermingled with motoneurons in the five studied nuclei (Fig. 2). Their general appearance resembled resting microglial cells. In none of the motor nuclei was a high intensity of VEGF expression by microglial cells observed in normal animals.

Confocal analysis was performed to quantify VEGF labelling inside the microglial cells, and no differences were obtained when the percentage of VEGF positive microglial cells was compared between any of the five analyzes nuclei (ABD: 46.65 ± 2.88 %; TRO: 27.28 ± 5.17 %, OCM: 38.04 ± 5.6 %, facial: 34.09 ± 4.52 %, hypoglossal: 32.83 ± 4.29 %; one-way ANOVA test; $p > 0.05$; $n = 4$; Fig. 2j).

Taken together, these results of VEGF expression by glial cells in basal conditions suggest that the differences observed in VEGF levels in brainstem motoneurons are not due to differences in VEGF supply from their surrounding glial cells.

3.3. Expression of VEGF and Flk-1 by target muscles to brainstem motoneurons.

Another possible source of VEGF for motoneurons is target muscle. Extraocular, buccinator and tongue muscles were analyzed, as targets of oculomotor, facial and hypoglossal motoneurons, respectively. Western blot analysis was performed to quantify the amount of VEGF and Flk-1 protein present in the target muscles. In addition, we studied VEGF location inside these muscles by means of immunohistochemistry, in order to see whether that trophic factor was present in the muscle fibers, and the location of its Flk-1 receptor in the axon terminals of the projecting motoneurons.

Data of VEGF or Flk-1 expression obtained from extraocular muscles were considered as 1, and data obtained from buccinator or tongue muscles were relativized to those. For VEGF, the band of 45 kDa corresponding to the molecular size of the neurotrophic factor was analyzed and protein expression was compared between muscles (Fig. 3a). The analysis showed that all of the studied muscles contained VEGF protein. Despite optical density of VEGF protein measured in the buccinator (1.90 ± 0.39) and tongue (1.48 ± 0.26) muscles, innervated by facial and hypoglossal nerves, respectively, were apparently higher than that measured in the extraocular muscles (relativized to 1), no significant differences were detected between them (one-way ANOVA test; $p > 0.05$; $n = 6$; Fig. 3b).

For Flk-1, a band corresponding to a molecular weight of 150 kDa was analyzed (Fig. 3c). In this case, the analyses yielded the following result: the presence of the Flk-1 protein was significantly higher in

the extraocular muscles (relativized to 1), than in buccinator (0.45 ± 0.05) or tongue muscles (0.53 ± 0.07) (*: one-way ANOVA test; $p < 0.001$; $n = 6$; Fig. 3d).

Therefore, all the analyzed muscles contained VEGF and consequently could act as sources of the trophic factor for the motoneurons that innervate them. On the other hand, the extraocular muscle showed a higher concentration of the Flk-1 receptor than the other two cranial muscles.

To study the distribution of VEGF in the target muscles, extraocular, buccinator and tongue muscles were dissected and sectioned after perfusion. An antibody against VEGF was used, together with phalloidin, to label the muscle fibers, and DAPI, to label the cellular nuclei. As it can be seen in Fig. 4a, b, f, g, k, l, VEGF was present in the muscle fibers of every of the muscles analyzed. Optical density of VEGF immunolabelling was measured in extraocular muscles (21.98 ± 2.72), buccinator (21.65 ± 5.08) and tongue muscle (15.55 ± 2.07). When optical density of VEGF signal was compared between muscles, no significant differences were obtained (one-way ANOVA test; $p > 0.05$; $n = 4$; Fig. 4p).

In another set of muscle tissues, immunohistochemistry was performed to detect expression of Flk-1 in axon terminal. The presynaptic terminal of the neuromuscular junction was identified by the labelling with anti-NeuM, and the postsynaptic portion by labelling with α-bungarotoxin. As shown in Fig. 4c-e, h-j and m-o, the Flk-1 signal (pseudocolored in white) was located between the axon (identified by NeuM, in green) and the postsynaptic element (stained with α-bungarotoxin, in red). After confocal and quantitative analysis of Flk-1 at the presynaptic elements, a greater quantity of the receptor was located in the axon terminals of ocular motoneurons (mean optical density: 2.78 ± 0.53), compared to facial (1.22 ± 0.25) or hypoglossal (0.88 ± 0.20) motoneurons (*: one-way ANOVA test; $p < 0.05$; $n = 4$; Fig. 4q).

Thus, although VEGF expression was similar in the three muscles, the amounts of Flk-1 were higher at the extraocular muscles compared to the buccinator and tongue muscles, and the receptor was located preferentially in the axon terminal. The fact that the terminals of the nerves innervating extraocular muscles showed more Flk-1 suggests that these terminals had a greater sensitivity to VEGF and would be capable of binding and internalizing greater quantities of VEGF, even though the VEGF concentration in the extraocular muscles was no greater than in the buccinator or tongue. Taken together, these results indicate that VEGF could be acting as a retrograde neurotrophic factor for brainstem motoneurons in general, but its importance is more notable for motoneurons of the ocular motor system in particular.

3.4. VEGF and Flk-1 expression in cells of the brainstem motor nuclei after axotomy

We aimed to study how VEGF and its Flk-1 receptor were regulated in cells located in the brainstem nuclei, i.e., motoneurons, astrocytes and microglial cells, in response to lesion. Axotomy of cranial nerves was performed as a method to deprive motoneurons from target muscles, and it also interrupted the VEGF retrograde supply from muscles cells. In order to induce the axotomy and its consequent glial reaction, the nerves innervating extraocular, facial and tongue muscles were sectioned in separated groups of animals. One week after the axotomy, tissue was analyzed by means of qPCR and immunohistochemistry.

3.4.1. Change in VEGF and Flk-1 mRNA expression in the brainstem motor nuclei after axotomy.

After axotomy, we quantified the expression of VEGF in the axotomized nuclei, and made comparisons with their respective control sides by means of qPCR. mRNA was extracted from control and lesioned oculomotor complex, as well as facial and hypoglossal nuclei. VEGF mRNA expression of the control side was considered as 100 %, and expression in the axotomized side was compared to this value. There was a significant decrease in VEGF mRNA in the facial (62.43 ± 9.24 %) and hypoglossal (62.79 ± 3.99 %) nuclei in response to motoneuron axotomy (*: paired t-tests control *vs*. lesioned side; $p < 0.05$). However, this reduction was not observed in the oculomotor complex (103.95 ± 11.85 %; paired t-test; $p > 0.05$). The effect of axotomy in VEGF mRNA expression was also compared between nuclei. Significant differences were observed between oculomotor complex and facial and hypoglossal nuclei (#: one-way ANOVA test; $p < 0.005$; $n = 6$; Fig. 5a).

Similarly, we also compared the expression of Flk-1 mRNA between intact and lesioned oculomotor complex, facial and hypoglossal nuclei. Flk-1 mRNA in the control nuclei was considered as

100 %, and expression in injured nuclei was expressed related to their respective control sides. Again, one week after motoneuron axotomy, there was a significant reduction in the expression of Flk-1 in both the facial (58.28 ± 6.29 %) and hypoglossal (67.95 ± 4.89 %) nuclei (*: paired t-tests; $p < 0.05$). In contrast to these results, Flk-1 expression did not change in the oculomotor complex (107.83 ± 10.12 %; paired t-test; $p > 0.05$). The percentage of change as a result of the axotomy was significantly different between facial and hypoglossal nuclei compared to oculomotor nucleus (#: one-way ANOVA test; $p < 0.001$; $n = 6$; Fig. 5b).

Therefore, these qPCR results showed that, although no higher expression of VEGF mRNA or Flk-1 mRNA was observed on the injured side of the oculomotor complex, a decrease in the expression of VEGF or Flk-1 mRNA in the facial and hypoglossal nuclei in response to injury was quantified. These results imply that facial and hypoglossal motoneurons are less exposed to the beneficial effect of internally generated VEGF after axotomy. Changes observed in the expression of VEGF and its receptor after lesion could be due to variations in the trophic factor expression by motoneurons or by glial cells, astrocytes or microglial cells. We performed immunohistochemistry to examine the cellular changes in those three types of cells located in the brainstem nuclei.

3.4.2. Variations in VEGF and Flk-1 protein expression in motoneurons of brainstem motor nuclei in response to axotomy.

Double immunohistochemical labelling was used to detect variations in VEGF and Flk-1 protein expression in the brainstem motoneurons after axotomy. As it can be appreciated in Fig. 6, VEGF immunostaining was higher on the control side in ocular motoneurons (Fig. 6a-b) compared to control side facial and hypoglossal motoneurons (Fig. 6e-f and 6i-j, respectively), as we have previously described (Silva-Hucha et al., 2017). After motoneuronal axotomy, a significant increase in VEGF presence could be observed in axotomized motoneurons of the ocular motor system compared to control neurons (ABD: 183.36 ± 21.65 %, TRO; 213.29 ± 17.31 % and OCM: 197.39 ± 15.89 %; *: paired t-tests; $p < 0.05$; Fig. 6b *vs.* 6d). However, in facial and hypoglossal motoneurons no increase in the trophic factor expression was found after axotomy (79.25 ± 6.57 % and 97.70 ± 6.68 %, respectively; paired t-tests; $p > 0.05$; Fig. 6f *vs*. 6h, and 6j *vs.* 6l). Thus, there was a significantly different response in ocular motoneurons compared to the other brainstem nuclei studied with respect to VEGF expression following axotomy (#: one-way ANOVA test; $p < 0.001$; $n = 4$; Fig. 6m). Note the reduction in ChAT expression displayed by the axotomized motoneurons seven days after axotomy (Fig. 6c, g and k).

Flk-1 expression was also studied after axotomy in motoneurons, in order to see if those cells experienced a change in the expression of the VEGF receptor in response to injury (Fig. 7 a-l). When the intensity of Flk-1 immunolabelling was compared between control and lesioned motoneurons, a significant increase was observed in ocular injured motoneurons (ABD: 149.47 ± 7.90 %, TRO; 238.36 ± 22.08 % and OCM: 181.67 ± 7.55 %; *: paired t-tests; $p < 0.05$; Fig. 7b *vs.* 7d). Again, no differences were obtained when Flk-1 expression was compared between facial and hypoglossal motoneurons of injured *versus* control side (96.13 ± 12.57 % and 70.82 ± 12.38 %, respectively; paired t-tests; $p > 0.05$; Fig. 7f *vs*. 7h, and 7j *vs.* 7l). Hence, the motoneurons of the ocular motor system responded to injury by significantly increasing Flk-1 expression, but facial and hypoglossal motoneurons did not (#: one-way ANOVA test; $p < 0.001$; $n = 4$; Fig. 7m).

3.4.3. Variations in VEGF protein expression in astrocytes and microglial cells of brainstem motor nuclei in response to axotomy.

Triple immunohistochemistry labelling was employed to detect variations in VEGF protein expression in the glial cells inside the brainstem nuclei after axotomy. A large astroglial reaction was observed in the five motor nuclei, compared to their respective control nucleus (Fig. 8, GFAP in white; a *vs*. c, e *vs.* g and i *vs.* k). In every studied nucleus, GFAP signal was significantly higher in the lesioned side with respect to control side nucleus (ABD: 537.33 ± 229.84 %, TRO: 375.77 ± 42.88 %, OCM: 986.42 ± 66.19 %, facial: 2976.12 ± 139.38 % and hypoglossal: 545.83 ± 133.09 %; *: paired t-tests; $p < 0.05$; Fig. 8m). However, when VEGF immunostaining was quantified in reactive astrocytes (Fig. 8, VEGF in green; b *vs*. d, f *vs*. h, and j *vs*. l), no significant differences were observed in any of the motor nuclei compared to their control side (ABD: 82.91 ± 32.21 %, TRO: 135.62 ± 53.38 %, OCM: 84.95 ± 11.58 %, facial: 88.36

± 6.64 % and hypoglossal: 115.63 ± 6.74 %; paired t-tests; $p > 0.05$; Fig. 8m), nor were differences observed between nuclei (one-way ANOVA test; $p > 0.05$; $n = 4$; Fig. 8m).

Microglial cells were also analyzed after axotomy. When Iba1 was used as a marker of microglial cells, an increase in this marker was observed in every nucleus after axotomy (Fig. 9, Iba1 in white; a *vs.* c, e *vs.* g and i *vs.* k). Fig. 9m represents those differences between axotomized nuclei with respect to their respective control side (ABD: 504.81 ± 167.02 %, TRO: 253.31 ± 24.16 %, OCM: 162.35 ± 23.33 %, facial: 1119.39 ± 127.44 % and hypoglossal: 656.67 ± 193.84 %; *: paired t-tests; $p < 0.05$). VEGF expression in this cellular type was low in the nuclei studied, even after axotomy (Fig. 9, VEGF in green; d *vs.* b, h *vs.* f and l *vs.* j). Moreover, no significant differences were found in any of the brainstem nuclei between control and lesioned side (ABD: 119.29 ± 19.96 %, TRO: 77.95 ± 10.64 %, OCM: 74.30 ± 13.28 %, facial: 37.51 ± 13.96 % and hypoglossal: 58.54± 18.16 %; paired t-tests; $p > 0.05$; Fig. 9 m). When VEGF expression in the microglial cells of the five nuclei were compared with each other, no differences were observed (one-way ANOVA test; $p > 0.05$; $n = 4$; Fig. 9m).

Therefore, only the motoneurons of oculomotor nuclei modified their expression of VEGF and Flk-1 in response to axotomy. Thus, the motoneurons of the ocular motor system have the ability to modify their VEFG and Flk-1 level in an adverse situation. No change was produced in VEGF expression by glial cells after axotomy, suggesting once again that these types of cells (astrocytes or microglial cells) do not seem to be the main source of the VEGF for brainstem motoneurons. So they are unlikely to be key actors in modulating motoneuron resistance to injury through this mechanism or to be responsible for differences in injury response between different populations of brainstem motoneurons. Table 1 is included summarizing the intensity of VEGF labelling detected in the different cell types in a control situation and after axotomy.

4. Discussion

The central purpose of this work has been to evaluate the main sources of VEGF which could contribute to the greater amount of the trophic factor found in the soma of motoneurons innervating extraocular muscles, since this protein seems to be contributing to their higher resistance to degeneration. Our results show that the target muscles and the motoneurons themselves appear to be the main sources of VEGF for brainstem motoneurons, rather than glial cells.

Our second objective has been to uncover how cells in different brainstem motor nuclei responds to injury, in relation to their expression of VEGF. In this study, we have found a strong upregulation of VEGF in motoneurons of the ocular motor system, which was not present in the motoneurons of facial and hypoglossal nuclei. This modulation was not apparent in the glia of any of the nuclei examined.

4.1. Glial cells are not the main source of VEGF for brainstem motoneurons

We have observed that under normal conditions, the presence of VEGF in the astrocytes and in the microglia cells of brainstem motor nuclei is very weak (McCloskey et al., 2008; Silva-Hucha et al., 2017). Previous studies have also indicated that glial cells in the intact central nervous system do not express large amounts of VEGF (Krum and Rosenstein, 1998), apart from astrocytes of the subventricular zone (Tonchev et al., 2007). This strongly suggests that the VEGF present in intact brainstem motoneurons is not supplied by glial cells. Therefore, a paracrine relationship between glia and motoneurons does not seem to be contributing to the different levels of VEGF observed in the distinct pool of cranial motoneurons. However, glial cells can modify their VEGF expression in adverse conditions (Bartholdi et al., 1997; Lennmyr et al., 1998; Sköld et al., 2000; Argaw et al., 2012), thus, we aimed to uncover if the expression of the trophic factor is altered in astrocytes or microglial cells in our model of axotomy of cranial nerves.

4.2. VEGF is presents in all the cranial muscles studied, acting as a retrograde source for brainstem motoneurons

Target muscles are classically considered a trophic factor source for motoneurons. Motoneurons are dependent on neurotrophic factors derived from their target muscles for survival and for the maintenance

of their synaptic and molecular characteristics (Purves, 1990; Gould and Oppenheim, 2011; Morcuende et al., 2013), particularly during development. By contract, adult motoneurons survive in a great proportion after the deprivation of the target muscles, but they experience changes in their physiology, such as a decrease in the expression of ChAT or alterations in their electrophysiological properties (Navarro et al., 2007; Morcuende et al., 2013). It is noteworthy that these characteristics are largely recovered after neurotrophic factor administration (Davis-López de Carrizosa et al., 2009, 2010).

All the cranial muscles analyzed in this work express a high amount of VEGF. Thus, these muscles are good candidates to be acting as a retrograde source of VEGF for motoneurons. Muscle fibers in other muscles have been previously reported to be enriched with VEGF (Hoier and Hellsten, 2014), and it has been proven that this neurotrophic factor can be retrogradely transported from muscle to motoneuron somata (Storkebaum et al., 2005), retarding spinal cord motoneuronal death after its administration in muscle (Azzouz et al., 2000). Therefore, our results strongly suggest that the VEGF observed in cranial muscles is acting as a source of support for brainstem motoneurons following receptor mediated uptake and transport.

4.3. Synaptic terminals of motoneurons innervating extraocular muscles are enriched in Flk-1 receptor

Despite of being positive for VEGF, not all the target muscles seem to be as effective as a source of VEGF for supporting the motoneurons that innervate them. Specifically, this study suggests that particular motoneuron populations may receive a different trophic contribution depending on the concentration of VEGF receptors they have at their synaptic terminals. We have quantified a higher density of Flk-1 in the synaptic terminal of the motoneurons that innervate the extraocular muscles. This may provide a mechanism for increasing the amount of retrogradely transported VEGF in this population, despite the fact that the extraocular muscles themselves do not contain significantly greater levels of VEGF. In this way, extraocular muscles may have a greater influence on ocular motoneurons that the muscles targeted by other cranial motoneurons have on these motor nuclei.

Indeed, previous reports have shown the presence of the Flk-1 receptor at the neuromuscular junction level of the abducens axons (Calvo et al., 2018a). Recently, intramuscular injection of VEGF has been reported to increase regeneration after nerve crush (Guy et al., 2019). Therefore, differences in Flk-1 presence in the neuromuscular junction may help explain differences in response to neurodegeneration among brainstem motor nuclei.

4.4. VEGF and Flk-1 increase in motoneurons of the ocular motor system in response to axotomy

One of the most important observations of this study is that axotomy produced a significant increase in the presence of VEGF in the soma of the motoneurons innervating extraocular muscles, but not in facial or hypoglossal motoneurons. Previous studies have shown modifications in trophic factor and its receptors in motoneurons after axotomy (Koliatsos et al., 1991; Kobayashi et al., 1996; Morcuende et al., 2011).

The upregulation of VEGF, and also Flk-1, described in ocular motoneurons has been detected by immunohistochemistry. However, data from qPCR experiments showed no significant increase in mRNA VEGF expression in nuclei of the oculomotor system. At this point, it should be noted that the tissue extracted from the nuclei to be analyzed by qPCR includes both the motoneurons and the glial cells contained in the nuclei. Since an upregulation in VEGF in glial cells was not observed, that could partially mask the results observed only in motoneurons by immunohistochemistry. Given that axotomized motoneurons have not got a retrograde source of trophic factors, and surrounding glia does not seem to be the VEGF source either, the most likely explanation for the raise in VEGF protein content could be existence of changes in post-transcriptional regulation. The same logic could be applied in the case of facial and hypoglossal motoneurons, where a drop in VEGF mRNA content does not coincide with a reduction in VEGF protein. Post-transcriptional regulation of protein synthesis has received increasing interest in the last years, since this regulation may affect each step from mRNA transcription to the final protein translation, including mRNA splicing, poliadenylation, transport outside the nucleus, cytoplasm storage vs. rapid degradation and the initial point of translation (Vlasova-St. Louis and Bohjanen, 2017). Cytokine and trophic factor expression is typically regulated at posttranscriptional stages. More precisely, VEGF has

been demonstrated to be regulated at each of these possible steps (Arcondéguy et al., 2013) and thus, in the case of the oculomotor nucleus, it could be possible that the same amount of mRNA molecules could be translated into a greater number of protein molecules.

In addition, it is worth noting several considerations: i) to study the response of VEGF or Flk-1 mRNA in brainstem motor nuclei, we extracted tissue from the oculomotor complex, that apart from the oculomotor nucleus, also include the trochlear (Haenggeli and Kato, 2002); ii) enucleation, i.e., axotomy of extraocular nerves, was performed unilaterally; iii) the oculomotor nucleus contains four subnuclei of motoneurons, three ipsilateral and one contralateral for a given eye (Büttner and Büttner-Ennever, 2006; Morcuende et al., 2011), meanwhile motoneurons of the trochlear nucleus project to the contralateral target muscle. As a result, two of the five subpopulations of extraocular motoneurons of the control side are affected by axotomy, meanwhile two subpopulations of the lesioned side remain intact. That situation would contribute again to minimize the changes in VEGF or Flk-1 mRNA quantified in the oculomotor complex between control and axotomized sides, which are clearly observed at cellular level by immunohistochemistry.

Upregulation of VEGF seems to be a common phenomenon observed in a diverse type of neural tissues after insults, and it has been linked to neuroprotection (McCloskey et al., 2008; Nicoletti et al., 2008; Castañeda-Cabral et al., 2017). Thus, the ability of motoneurons to produce endogenous VEGF is important in maintaining the health of brainstem and spinal motoneurons (McCloskey et al., 2008). Motoneurons are especially vulnerable to degeneration due to several factors, such as their high sensibility to glutamate excitotoxicity, because of their low expression of the GluA2 AMPA (formerly GluR2) receptor subunit (Medina et al., 1996; Van Den Bosch et al., 2000; Bogaert et al., 2010), which makes these receptors permeable to calcium. However, motoneurons of the oculomotor system show a greater buffering capacity because they are enriched in the Ca^{2+} buffering proteins parvalbumin and calbindin D-28K (Alexianu et al., 1994; Reiner et al., 1995; von Lewinski and Keller, 2005), which could contribute, along with other factors, to their greater resistance. High levels of VEGF induce an increase in GluA2 levels on motoneurons (Bogaert et al., 2010). Therefore the capacity of these motoneurons to respond to damage increasing VEGF, together with the fact that this particular motoneuronal population exhibits a high calcium buffering capacity (Alexianu et al., 1994; Vanselow and Keller, 2000; Brockington et al., 2013), could lead to a neuroprotective effect.

Axotomy of the facial and hypoglossal nerves are classic and well characterized models of nerve injury (Olmstead et al., 2015). Eye enucleation has also been widely used as an axotomy model for extraocular nerves (Morcuende et al., 2005). One might think that this approach is more invasive than facial and hypoglossal axotomy, but in turn, the cutting of the nerve occurs more distally, near the target muscle, thus minimizing damage to the motor neuron, constituting a model of injury of comparable severity.

Most survival effects of VEGF on motoneurons are mediated by Flk-1 (Sköld et al., 2000; Storkebaum et al., 2004; Pronto-Laborinho et al., 2014), and the expression of this receptor is decreased in spinal motoneurons of G93A-SOD1 ALS mice (Lunn et al., 2009), causing neurodegeneration. In line with this, a reduction in other neurotrophic receptors has been described in the neuromuscular junction of limb muscles in ALS transgenic mice, which was not observed in extraocular muscles (Harandi et al., 2016).

Therefore, the increase of Flk-1 expression seen after axotomy in motoneurons innervating extraocular muscles, which is known to decrease apoptosis by activation of PI3K/Akt signaling via that receptor (Sondell et al., 2000), could make those neurons more receptive for VEGF and increase their resistance to degeneration.

4.5. No changes are induced in VEGF expression by glial cells after axotomy

Despite the induction of an axotomy, which may cause a change in the expression pattern of trophic factors in the nerve cells of the injured motor nuclei, no significant increase in VEGF production was observed in the glia cells of brainstem nuclei after axotomy. Increase in VEGF in astrocytes after different models of brain injury has been previously described. This response was produced by exposition to radiation (Bartholdi et al., 1997; Zhou et al., 2019), freeze lesions (Papavassiliou et al., 1997) or after brain trauma (Sköld et al., 2005). It peaks between 3 and 6 days after injury. Most brain injuries produce hypoxia as a secondary effect, and therefore, the upregulation of VEGF expression is preceded by an increased production of the hypoxia inducible factor 1 (HIF1α). A high VEGF induction in the neuropil surrounding damage could also be followed by an increase in vascular permeability, exacerbating blood-brain barrier

disruption, due to the role of VEGF in vascular permeability, increasing brain damage and compromising central nervous system homeostasis (Nordal et al., 2004; Ruiz de Almodovar et al., 2009; Li et al., 2014; Lange et al., 2016; Cárdenas-Rivera et al., 2019). Thus, a large induction on VEGF in the glial scar might not be beneficial for recovery after brain insults.

In other injury models, such as the model for stroke using occlusion of the middle cerebral artery, VEGF does not increase in astrocytes, but it does increase in microglial cells (Plate et al., 1999). That upregulation was observed shortly after injury, that is, in hours, returning to basal levels by one week. It is worthy to indicate that VEGF interact with microglial cells preferentially via Flt-1, instead of Flk-1 (Cárdenas-Rivera et al., 2019). Such an early, temporary change would not have been seen in our study.

We had expected to find an increase in VEGF expression in both astrocytes and microglia cells, since both cell types multiplied in response to the axotomy and presented a reactive phenotype. The fact that we did not observe that modification could be due to either the survival time, with ours being longer than many other experiments (Papavassiliou et al., 1997; Sköld et al., 2000) or to our lesion model, that induces a more localized lesion.

5. CONCLUSIONS

Our data suggest that the higher level of VEGF observed in motoneurons innervating extraocular muscles is mainly due to two sources: 1. the higher contribution of muscles as a retrograde source, caused by higher levels of Flk-1 in ocular motoneuron terminals, and 2. to higher levels the self-production by motoneurons, themselves. The low basal VEGF expression observed in astrocytes and microglial cells suggests that these cell types do not act as an important source of VEGF for brainstem motoneurons.

After axotomy, when the retrograde supply form the muscle is absent, motoneurons of the oculomotor system nevertheless respond by increasing VEGF and Flk-1 levels. This response is not seen in facial and hypoglossal motoneurons. Furthermore, even after the injury, the astrocytes and microglial cells of the affected nuclei do not increase their VEGF expression in this lesion model. Therefore, the upregulation of VEGF described in motoneurons of the oculomotor system appears to be an important factor for the survival of that pool of motoneurons under adverse conditions.

References

Acosta L, Morcuende S, Silva-Hucha S, Pastor AM, de la Cruz RR (2018) Vascular endothelial growth factor (VEGF) prevents the downregulation of the cholinergic phenotype in axotomized motoneurons of the adult rat. Front Mol Neurosci 11:241.

Alexianu ME, Ho B -K B-KK, Mohamed AH, La Bella V, Smith RG, Appel SH (1994) The role of calcium-binding proteins in selective motoneuron vulnerability in amyotrophic lateral sclerosis. Ann Neurol 36:846–858.

Arcondéguy T, Lacazette E, Millevoi S, Prats H, Touriol C (2013) VEGF-A mRNA processing, stability and translation: A paradigm for intricate regulation of gene expression at the post-transcriptional level. Nucleic Acids Res 41:7997–8010.

Argaw AT, Asp L, Zhang J, Navrazhina K, Pham T, Mariani JN, Mahase S, Dutta DJ, Seto J, Kramer EG, Ferrara N, Sofroniew M V., John GR (2012) Astrocyte-derived VEGF-A drives blood-brain barrier disruption in CNS inflammatory disease. J Clin Invest 122:2454–2468.

Azzouz M, Hottinger A, Paterna JC, Zurn AD, Aebischer P, Büeler H (2000) Increased motoneuron survival and improved neuromuscular function in transgenic ALS mice after intraspinal injection of an adeno-associated virus encoding Bcl-2. Hum Mol Genet 9:803–811.

Azzouz M, Ralph GS, Storkebaum E, Walmsley LE, Mitrophanous KA, Kingsman SM, Carmeliet P, Mazarakis ND (2004) VEGF delivery with retrogradely transported lentivector prolongs survival in a mouse ALS model. Nature 429:413–417.

706 Bartholdi D, Rubin BP, Schwab ME (1997) VEGF mRNA induction correlates with changes in the
707 vascular architecture upon spinal cord damage in the rat. Eur J Neurosci 9:2549–2560.

708 Benítez-Temiño B, Davis-López de Carrizosa MA, Morcuende S, Matarredona ER, de la Cruz RR, Pastor
709 AM (2016) Functional diversity of neurotrophin actions on the oculomotor system. Int J Mol Sci
710 17:2016.

711 Bogaert E, Van Damme P, Poesen K, Dhondt J, Hersmus N, Kiraly D, Scheveneels W, Robberecht W,
712 Van Den Bosch L (2010) VEGF protects motor neurons against excitotoxicity by upregulation of
713 GluR2. Neurobiol Aging 31:2185–2191.

714 Bogaert E, Van Damme P, Van Den Bosch L, Robberecht W (2006) Vascular endothelial growth factor in
715 amyotrophic lateral sclerosis and other neurodegenerative diseases. Muscle and Nerve 34:391–405.

716 Brockington A, Ning K, Heath PR, Wood E, Kirby J, Fusi N, Lawrence N, Wharton SB, Ince PG, Shaw
717 PJ (2013) Unravelling the enigma of selective vulnerability in neurodegeneration: Motor neurons
718 resistant to degeneration in ALS show distinct gene expression characteristics and decreased
719 susceptibility to excitotoxicity. Acta Neuropathol 125:95–109.

720 Büttner U, Büttner-Ennever JA (2006) Present concepts of oculomotor organization. Prog Brain Res
721 151:1–42.

722 Calvo PM, de la Cruz RR, Pastor AM (2018a) Synaptic loss and firing alterations in Axotomized
723 Motoneurons are restored by vascular endothelial growth factor (VEGF) and VEGF-B. Exp Neurol
724 304:67–81.

725 Calvo PM, Pastor AM, de la Cruz RR (2018b) Vascular endothelial growth factor: an essential
726 neurotrophic factor for motoneurons? Neural Regen Res 13:1181–1182.

727 Cárdenas-Rivera A, Campero-Romero AN, Heras-Romero Y, Penagos-Puig A, Rincón-Heredia R, Tovar-
728 y-Romo LB (2019) Early Post-stroke Activation of Vascular Endothelial Growth Factor Receptor 2
729 Hinders the Receptor 1-Dependent Neuroprotection Afforded by the Endogenous Ligand. Front
730 Cell Neurosci 13:270.

731 Castañeda-Cabral JL, Beas-Zarate C, Gudiño-Cabrera G, Ureña-Guerrero ME (2017) Glutamate Neonatal
732 Excitotoxicity Modifies VEGF-A, VEGF-B, VEGFR-1 and VEGFR-2 Protein Expression Profiles
733 During Postnatal Development of the Cerebral Cortex and Hippocampus of Male Rats. J Mol
734 Neurosci 63:17–27.

735 Croll SD, Goodman JH, Scharfman HE (2004) Vascular endothelial growth factor (VEGF) in seizures: a
736 double-edged sword. Adv Exp Med Biol 548:57–68.

737 Davis-López de Carrizosa MA, Morado-Díaz CJ, Morcuende S, de la Cruz RR, Pastor AM (2010) Nerve
738 growth factor regulates the firing patterns and synaptic composition of motoneurons. J Neurosci
739 30:8308–8319.

740 Davis-López de Carrizosa MA, Morado-Díaz CJ, Tena JJ, Benítez-Temiño B, Pecero ML, Morcuende S,
741 de la Cruz RR, Pastor AM (2009) Complementary actions of BDNF and neurotrophin-3 on the
742 firing patterns and synaptic composition of motoneurons. J Neurosci 29:575–587.

743 Devos D, Moreau C, Lassalle P, Perez T, De Seze J, Brunaud-Danel V, Destée A, Tonnel AB, Just N
744 (2004) Low levels of the vascular endothelial growth factor in CSF from early ALS patients.
745 Neurology 62:2127–2129.

746 Gould TW, Oppenheim RW (2011) Motor neuron trophic factors: therapeutic use in ALS? Brain Res Rev
747 67:1–39.

748 Guy R, Grynspan F, Ben-Zur T, Panski A, Lamdan R, Danon U, Yaffe D (2019) Human Muscle
749 Progenitor Cells Overexpressing Neurotrophic Factors Improve Neuronal Regeneration in a Sciatic
750 Nerve Injury Mouse Model. Front Neurosci 13:151.

751 Haenggeli C, Kato AC (2002) Differential vulnerability of cranial motoneurons in mouse models with

motor neuron degeneration. Neurosci Lett 335:39–43.

Harandi VM, Gaied ARN, Brännström T, Pedrosa Domellöf F, Liu J-X (2016) Unchanged Neurotrophic Factors and Their Receptors Correlate With Sparing in Extraocular Muscles in Amyotrophic Lateral Sclerosis. Invest Ophthalmol Vis Sci 57:6831–6842.

Hoier B, Hellsten Y (2014) Exercise-induced capillary growth in human skeletal muscle and the dynamics of VEGF. Microcirculation:301–314.

Ijichi A, Sakuma S, Tofilon PJ (1995) Hypoxia-induced vascular endothelial growth factor expression in normal rat astrocyte cultures. Glia 14:87–93.

Kobayashi NR, Bedard AM, Hincke MT, Tetzlaff W (1996) Increased expression of BDNF and trkB mRNA in rat facial motoneurons after axotomy. Eur J Neurosci 8:1018–1029.

Koliatsos VE, Crawford TO, Price DL (1991) Axotomy induces nerve growth factor receptor immunoreactivity in spinal motor neurons. Brain Res 549:297–304.

Krakora D, Mulcrone P, Meyer M, Lewis C, Bernau K, Gowing G, Zimprich C, Aebischer P, Svendsen CN, Suzuki M (2013) Synergistic effects of GDNF and VEGF on lifespan and disease progression in a familial ALS rat model. Mol Ther 21:1602–1610.

Krum JM, Rosenstein JM (1998) VEGF mRNA and its receptor flt-1 are expressed in reactive astrocytes following neural grafting and tumor cell implantation in the adult CNS. Exp Neurol 154:57–65.

Lambrechts D et al. (2003) VEGF is a modifier of amyotrophic lateral sclerosis in mice and humans and protects motoneurons against ischemic death. Nat Genet 34:383–394.

Lange C, Storkebaum E, Ruiz De Almodóvar C, Dewerchin M, Carmeliet P (2016) Vascular endothelial growth factor: A neurovascular target in neurological diseases. Nat Rev Neurol 12:439–454.

Lennmyr F, Ata KA, Funa K, Olsoon Y, Terént A (1998) Expression of Vascular Endothelial Growth Factor (VEGF) and its receptors (Flt-1 and Flk-1) following permanent and transient occlusion of the middle cerebral artery in the rat. J Neuropathol Exp Neurol 57:874–882.

Li B, Xu W, Luo C, Gozal D, Liu R (2003) VEGF-induced activation of the PI3-K/Akt pathway reduces mutant SOD1-mediated motor neuron cell death. Mol Brain Res 111:155–164.

Li YN, Pan R, Qin XJ, Yang WL, Qi Z, Liu W, Liu KJ (2014) Ischemic neurons activate astrocytes to disrupt endothelial barrier via increasing VEGF expression. J Neurochem 129:120–129.

Lladó J, Tolosa L, Olmos G (2013) Cellular and molecular mechanisms involved in the neuroprotective effects of VEGF on motoneurons. Front Cell Neurosci 7:181.

Lunn JS, Sakowski SA, Kim B, Rosenberg AA, Feldman EL (2009) Vascular endothelial growth factor prevents G93A-SOD1-induced motor neuron degeneration. Dev Neurobiol 69:871–884.

McCloskey DP, Hintz TM, Scharfman HE (2008) Modulation of vascular endothelial growth factor (VEGF) expression in motor neurons and its electrophysiological effects. Brain Res Bull 76:36–44.

Medina L, Figueredo-Cardenas G, Rothstein JD, Reiner A (1996) Differential abundance of glutamate transporter subtypes in amyotrophic lateral sclerosis (ALS)-vulnerable versus ALS-resistant brain stem motor cell groups. Exp Neurol 142:287–295.

Morcuende S, Benítez-Temiño B, Pecero ML, Pastor AM, de la Cruz RR (2005) Abducens internuclear neurons depend on their target motoneurons for survival during early postnatal development. Exp Neurol 195:244–256.

Morcuende S, Matarredona ER, Benítez-Temiño B, Muñoz-Hernández R, Pastor AM, De la Cruz RR, Pastor ÁM, De la Cruz RR (2011) Differential regulation of the expression of neurotrophin receptors in rat extraocular motoneurons after lesion. J Comp Neurol 519:2335–2352.

Morcuende S, Muñoz-Hernández R, Benítez-Temiño B, Pastor AM, de la Cruz RR (2013)

Neuroprotective effects of NGF, BDNF, NT-3 and GDNF on axotomized extraocular motoneurons in neonatal rats. Neuroscience 250:31–48.

Murakami T, Ilieva H, Shiote M, Nagata T, Nagano I, Shoji M, Abe K (2003) Hypoxic induction of vascular endothelial growth factor is selectively impaired in mice carrying the mutant SOD1 gene. Brain Res 989:231–237.

Navarro X, Vivó M, Valero-Cabré A (2007) Neural plasticity after peripheral nerve injury and regeneration. Prog Neurobiol 82:163–201.

Nicoletti JN, Shah SK, McCloskey DP, Goodman JH, Elkady A, Atassi H, Hylton D, Rudge JS, Scharfman HE, Croll SD (2008) Vascular endothelial growth factor is up-regulated after status epilepticus and protects against seizure-induced neuronal loss in hippocampus. Neuroscience 151:232–241.

Nimchinsky EA, Young WG, Yeung G, Shah RA, Gordon JW, Bloom FE, Morrison JH, Hof PR (2000) Differential vulnerability of oculomotor, facial, and hypoglossal nuclei in G86R superoxide dismutase transgenic mice. J Comp Neurol 416:112–125.

Nordal RA, Nagy A, Pintilie M, Wong CS (2004) Hypoxia and hypoxia-inducible factor-1 target genes in central nervous system radiation injury: A role for vascular endothelial growth factor. Clin Cancer Res 10:3342–3353.

Ogunshola OO, Antic A, Donoghue MJ, Fan SY, Kim H, Stewart WB, Madri JA, Ment LR (2002) Paracrine and autocrine functions of neuronal vascular endothelial growth factor (VEGF) in the central nervous system. J Biol Chem 277:11410–11415.

Olmstead DN, Mesnard-hoaglin NA, Batka RJ, Haulcomb MM, Miller WM, Jones KJ (2015) Facial Nerve Axotomy in Mice : A Model to Study Motoneuron Response to Injury. J Vis Exp 96:1–7.

Oosthuyse B et al. (2001) Deletion of the hypoxia-response element in the vascular endothelial growth factor promoter causes motor neuron degeneration. Nat Genet 28:131–138.

Papavassiliou E, Gogate N, Proescholdt M, Heiss JD, Walbridge S, Edwards NA, Oldfield EH, Merrill MJ (1997) Vascular endothelial growth factor (vascular permeability factor) expression in injured rat brain. J Neurosci Res 49:451–460.

Plate KH, Beck H, Danner S, Allegrini PR, Wiessner C (1999) Cell type specific upregulation of vascular endothelial growth factor in an MCA-occlusion model of cerebral infarct. J Neuropathol Exp Neurol 58:654–666.

Pronto-Laborinho AC, Pinto S, de Carvalho M (2014) Roles of Vascular Endothelial Growth Factor in Amyotrophic Lateral Sclerosis. Biomed Res Int 947513:1–24.

Purves D (1990) Body and brain: a trophic theory of neural connections. Cambridge: Harvard University Press.

Reiner A, Medina L, Figueredo-Cardenas G, Anfinson S (1995) Brainstem motoneuron pools that are selectively resistant in amyotrophic lateral sclerosis are preferentially enriched in parvalbumin: evidence from monkey brainstem for a calcium-mediated mechanism in sporadic ALS. Exp Neurol 131:239–250.

Ruiz de Almodovar C, Lambrechts D, Mazzone M, Carmeliet P, Almodovar CRDE, Lambrechts D, Mazzone M (2009) Role and Therapeutic Potential of VEGF in the Nervous System. Physiol Rev 89:607–648.

Sathasivam S (2008) VEGF and ALS. Neurosci Res 62:71–77.

Senger D, Galli S, Dvorak A, Perruzzi C, Harvey V, Dvorak H (1983) Tumor cells secrete a vascular permeability factor that promotes accumulation of ascites fluid. Science (80-) 219:983–985.

Silva-Hucha S, Hernández RG, Benítez-Temiño B, Pastor AM, de la Cruz RR, Morcuende S (2017) Extraocular motoneurons of the adult rat show higher levels of vascular endothelial growth factor

and its receptor Flk-1 than other cranial motoneurons. PLoS One 12:e0178616.

Sköld M, Cullheim S, Hammarberg H, Piehl F, Suneson A, Lake S, Sjögren A, Walum E, Risling M (2000) Induction of VEGF and VEGF receptors in the spinal cord after mechanical spinal injury and prostaglandin administration. Eur J Neurosci 12:3675–3686.

Sköld MK, von Gertten C, Sandberg-Nordqvist A-C, Mathiesen T, Holmin S (2005) VEGF and VEGF receptor expression after experimental brain contusion in rat. J Neurotrauma 22:353–367.

Sondell M, Sundler F, Kanje M (2000) Vascular endothelial growth factor is a neurotrophic factor which stimulates axonal outgrowth through the flk-1 receptor. Eur J Neurosci 12:4243–4254.

Storkebaum E et al. (2005) Treatment of motoneuron degeneration by intracerebroventricular delivery of VEGF in a rat model of ALS. Nat Neurosci 8:85–92.

Storkebaum E, Lambrechts D, Carmeliet P (2004) VEGF: once regarded as a specific angiogenic factor, now implicated in neuroprotection. Bioessays 26:943–954.

Sun Y, Jin K, Xie L, Childs J, Mao XO, Logvinova A, Greenberg DA (2003) VEGF-induced neuroprotection, neurogenesis, and angiogenesis after focal cerebral ischemia. J Clin Invest 111:1843–1851.

Tolosa L, Mir M, Olmos G, Lladó J (2009) Vascular endothelial growth factor protects motoneurons from serum deprivation-induced cell death through phosphatidylinositol 3-kinase-mediated p38 mitogen-activated protein kinase inhibition. Neuroscience 158:1348–1355.

Tonchev AB, Yamashima T, Guo J, Chaldakov GN, Takakura N (2007) Expression of angiogenic and neurotrophic factors in the progenitor cell niche of adult monkey subventricular zone. Neuroscience 144:1425–1435.

Tovar-y-Romo LB, Tapia R (2012) Delayed administration of VEGF rescues spinal motor neurons from death with a short effective time frame in excitotoxic experimental models in vivo. ASN Neuro 4:121–129.

Van Den Bosch L, Vandenberghe W, Klaassen H, Van Houtte E, Robberecht W (2000) Ca2+-permeable AMPA receptors and selective vulnerability of motor neurons. J Neurol Sci 180:29–34.

Vanselow BK, Keller BU (2000) Calcium dynamics and buffering in oculomotor neurones from mouse that are particularly resistant during amyotrophic lateral sclerosis (ALS)-related motoneurone disease. J Physiol 525 Pt 2:433–445.

Vlasova-St. Louis I, Bohjanen PR (2017) Post-transcriptional regulation of cytokine and growth factor signaling in cancer. Cytokine Growth Factor Rev 33:83–93.

von Lewinski F, Keller BU (2005) Ca2+, mitochondria and selective motoneuron vulnerability: implications for ALS. Trends Neurosci 28:494–500.

Wang Y, Mao XO, Xie L, Banwait S, Marti HH, Greenberg DA, Jin K (2007) Vascular endothelial growth factor overexpression delays neurodegeneration and prolongs survival in amyotrophic lateral sclerosis mice. J Neurosci 27:304–307.

Zheng C, Nennesmo I, Fadeel B, Henter JI (2004) Vascular endothelial growth factor prolongs survival in a transgenic mouse model of ALS. Ann Neurol 56:564–567.

Zhou D, Huang X, Xie Y, Deng Z, Guo J, Huang H (2019) Astrocytes-derived VEGF exacerbates the microvascular damage of late delayed RBI. Neuroscience 408:14–21.

885
886
887
888
889
890
891
892
893
894
895
896
897
898
899
900
901
902
903
904
905
906
907
908
909
910
911
912
913

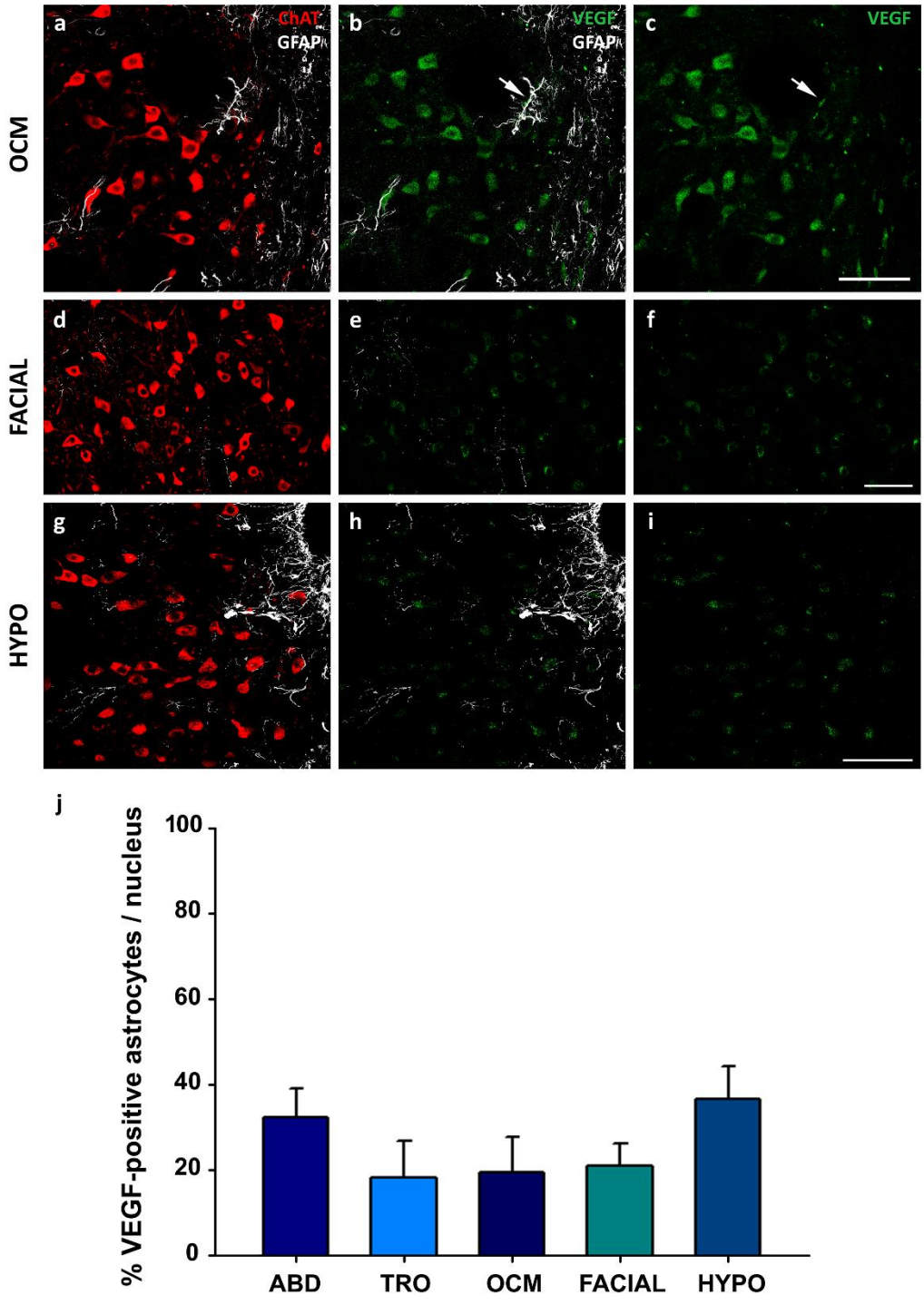

914

915 **Fig. 1**

916 VEGF immunoreactivity in astrocytes of cranial motor nuclei. In control situation, expression of VEGF (in
917 green) was low in astrocytes (labelled with an antibody against GFAP, pseudocolored in white). The
918 confocal images show the oculomotor nucleus (OCM; a-c), the facial nucleus (d-f), and the hypoglossal
919 nucleus (HYPO; g-i). Scale bars = 100 μm (in C for a-c; in f for d-f; in i for g-i). Arrows in b and c point
920 some examples of VEGF-positive astrocytes. (j) Quantification of the percentage of VEGF-positive
921 astrocytes in cranial motor nuclei showed no significant differences between them (one-way ANOVA test;
922 $p > 0.05$; $n = 4$ animals).

923

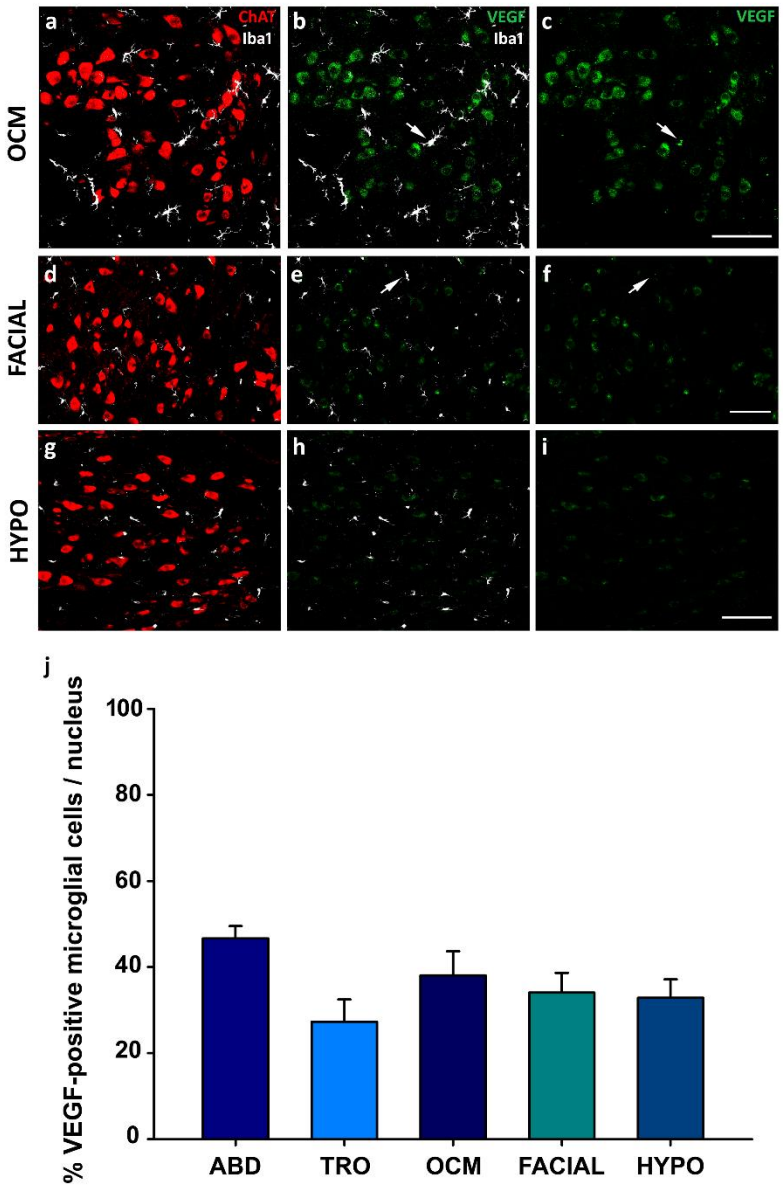

Fig. 2

VEGF immunoreactivity in microglial cells of cranial motor nuclei. In control situation, expression of VEGF (in green) was low in microglial cells (identified with an antibody against Iba1, pseudocolored in white). The confocal images show the oculomotor nucleus (OCM; a-c), the facial nucleus (d-f), and the hypoglossal nucleus (HYPO; g-i). Scale bars = 100 μm (in c for a-c; in f for d-f; in i for g-i). Arrows point some examples of VEGF-positive microglial cells. (j) Quantification of the percentage of VEGF-positive microglial cells in cranial motor nuclei showed no significant differences between them (one-way ANOVA test; $p > 0.05$; $n = 4$ animals).

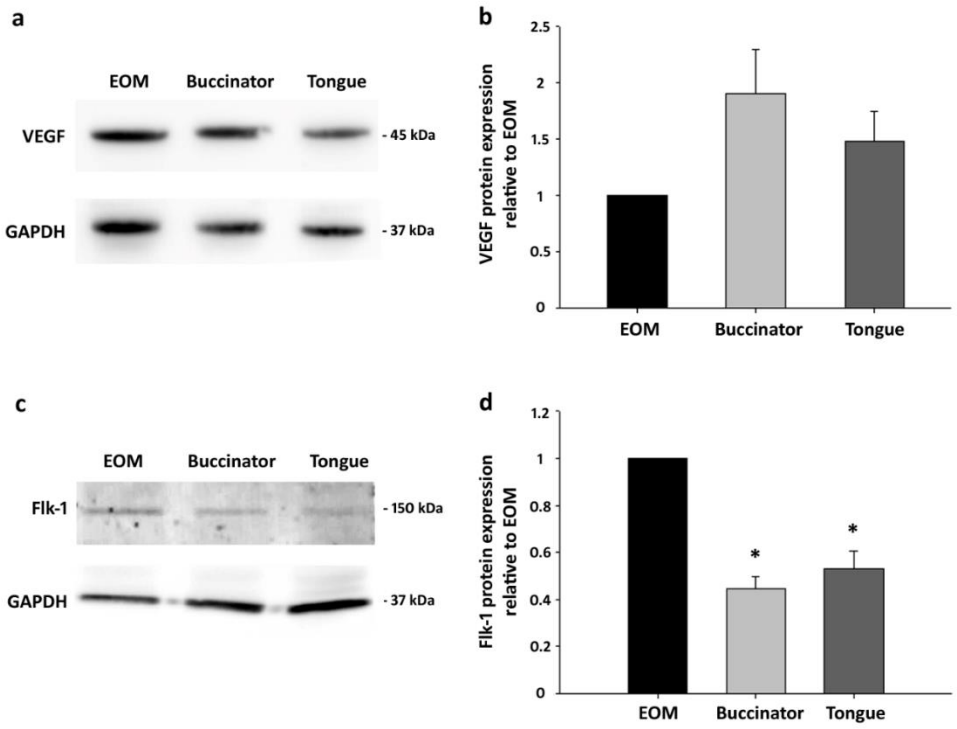

Fig. 3

Western blot analysis of VEGF and Flk-1 proteins in cranial muscles. (a) The protein band for VEGF is shown for the extraocular (EOM), buccinator and tongue muscles, target muscles for extraocular, facial and hypoglossal motoneurons, respectively. GAPDH immunoblotting was used as load control. (b) Densitometry data showed no significant differences in the amount of VEGF protein between the studied muscles (one-way ANOVA test followed by Holm-Sidak method for multiple pairwise comparisons; $p > 0.05$; $n = 6$ animals). (c) The band for Flk-1 protein is shown for the extraocular (EOM), buccinator and tongue muscles. GAPDH immunoblotting was used as load control. (d) Densitometry data showed a significantly higher amount of Flk-1 protein in extraocular muscles as compared to the buccinator and tongue muscles (*: significant differences with EOM; one-way ANOVA test; $p < 0.001$; $n = 6$ animals).

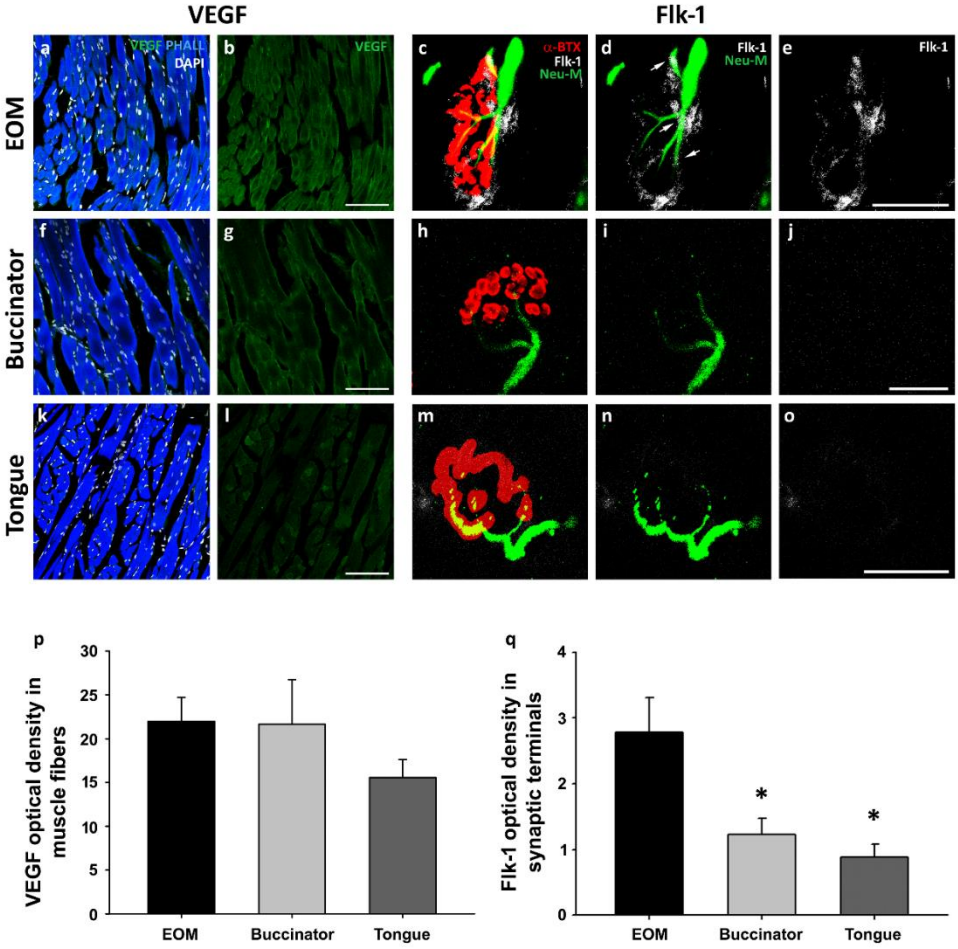

Fig. 4

Presence of VEGF and Flk-1 in cranial muscles. The confocal images show the presence of VEGF (in green; a-b, f-g and k-l) in target muscle cells (identified with an antibody against phalloidin, PHALL, blue; a, f and k). Cellular nuclei of muscle cells are labelled with DAPI (in white; a, f and k). In all the studied muscles VEGF was present. c-e, h-j and m-o images show end plate terminals of motoneurons. The postsynaptic element was identified by α-bungarotoxin (α-BTX, red; c, h and m), the axon of projecting motoneurons was labelled with an antibody against neurofilaments (NeuM, in green; c-d, h-i and m-n). Note the higher presence of the Flk-1 (pseudocolored in white) in the presynaptic terminal of the motoneurons innervating extraocular muscles (d-e) compared to facial and hypoglossal motoneurons (i-j and n-o, respectively). Arrows in D point to some examples of Flk-1 receptor labelling within the axon. Scale bars = 100 μm (in b for a-b; in e for c-e; in g for f-g; in j for h-j; in l for k-l; in o for m-o). VEGF and Flk-1 immunosignal was analyzed in the muscle cells and in presynaptic terminals, respectively. (p) No differences were observed in the VEGF immunolabelling between the different muscles (one-way ANOVA test, $p > 0.05$; $n = 4$ animals). (q) Histogram showing higher Flk-1 labelling in terminals of motoneurons of the oculomotor system than in facial and hypoglossal presynaptic terminals (*: significant differences with EOM; one-way ANOVA test; $p < 0.05$; $n = 4$ animals).

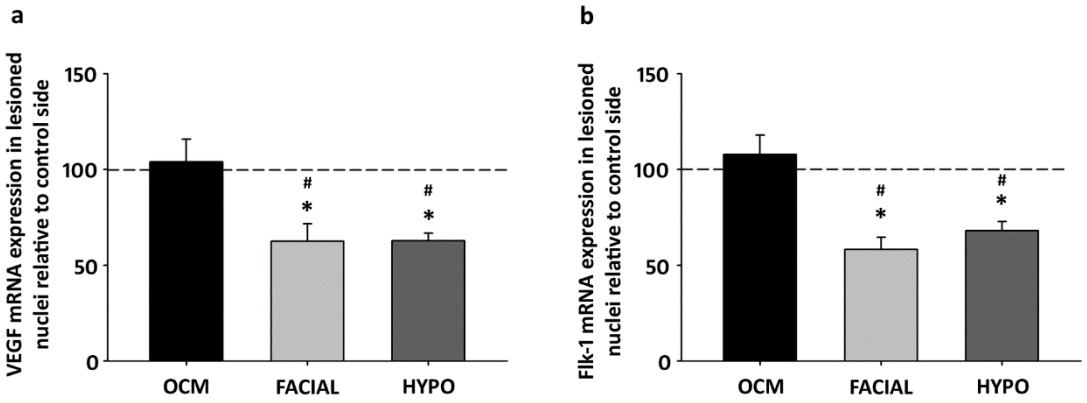

Fig. 5

VEGF and Flk-1 mRNA expression in cranial nuclei in response to axotomy. (a) Quantification of VEGF mRNA expression in lesioned nuclei compared to control side. No differences were obtained in oculomotor complex (OCM), but a significant decrease in VEGF mRNA expression was found in lesioned facial and hypoglossal nuclei compared to their respective control sides (*: significant differences to control side; paired t-tests; $p < 0.05$; #: significant differences to OCM; one-way ANOVA test; $p < 0.01$; $n = 6$ animals). (b) Quantification of Flk-1 mRNA expression in lesioned nuclei compared to control side. No differences were obtained in oculomotor complex (OCM), but again a significant decrease in Flk-1 mRNA expression was found in lesioned facial and hypoglossal nuclei compared to their respective control sides (*: significant differences to control side; paired t-tests; $p < 0.05$; #: significant differences to OCM; one-way ANOVA test; $p < 0.001$; $n = 6$ animals).

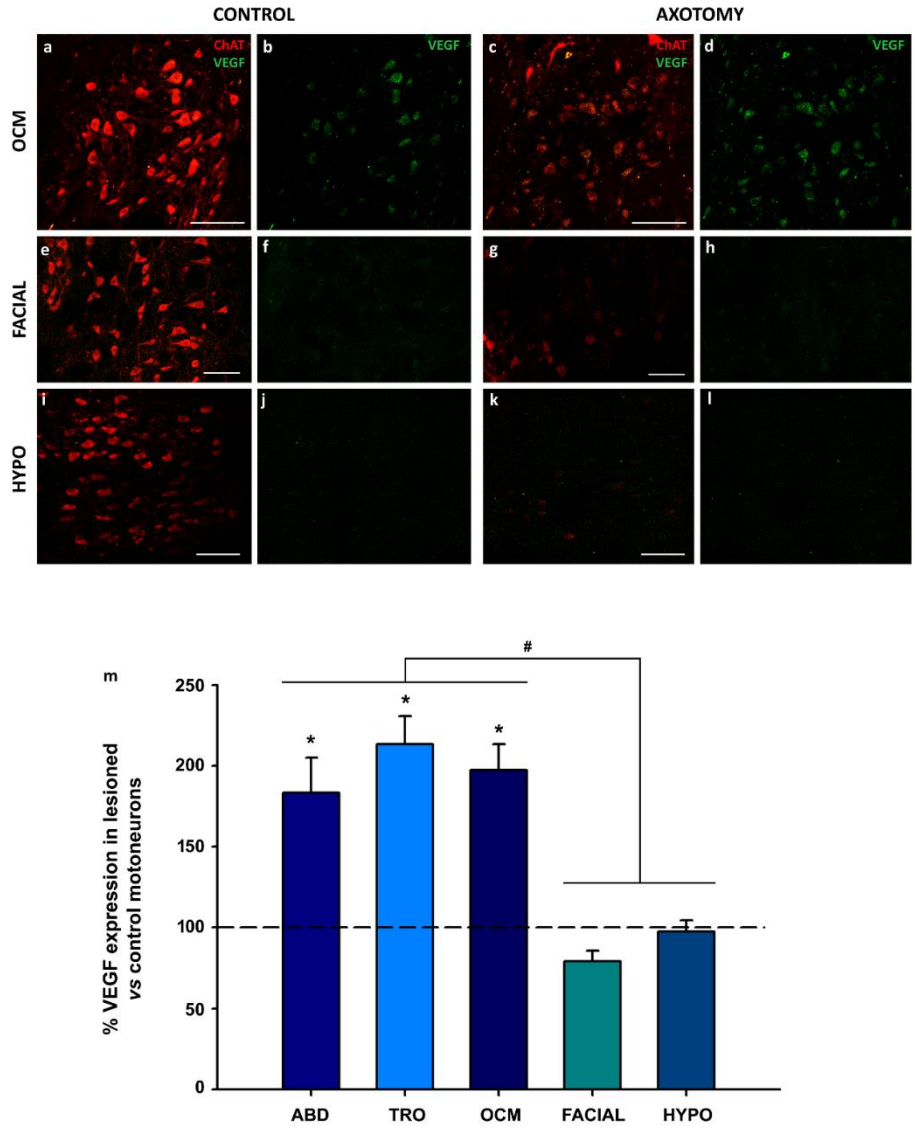

Fig. 6

VEGF immunoreactivity in brainstem motoneurons in response to axotomy. (a-d) VEGF (in green) increased in the soma of lesioned motoneurons of the oculomotor system (c-d) compared to control motoneurons (a-b). However, no increase was observed in lesioned facial (g-h) or hypoglossal (k-l) motoneurons compared to their control (e-f and i-j, respectively). Scale bars = 100 μm (in a for a-b; in c for c-d; in e for e-f; in g for g-h; in i for i-j; in k for k-l). Motoneurons were identified by ChAT antibody (in red). (m) Histogram showing higher VEGF labelling in the soma of lesioned motoneurons innervating extraocular muscles compared to their respective control motoneurons (*: paired t-tests; $p < 0.05$; $n = 4$ animals; significant differences to control side (= 100 %)). When the increase of VEGF in response to injury was compared between motoneurons of the different nuclei, significant differences were observed (#: one-way ANOVA test; $p < 0.001$; $n = 4$ animals).

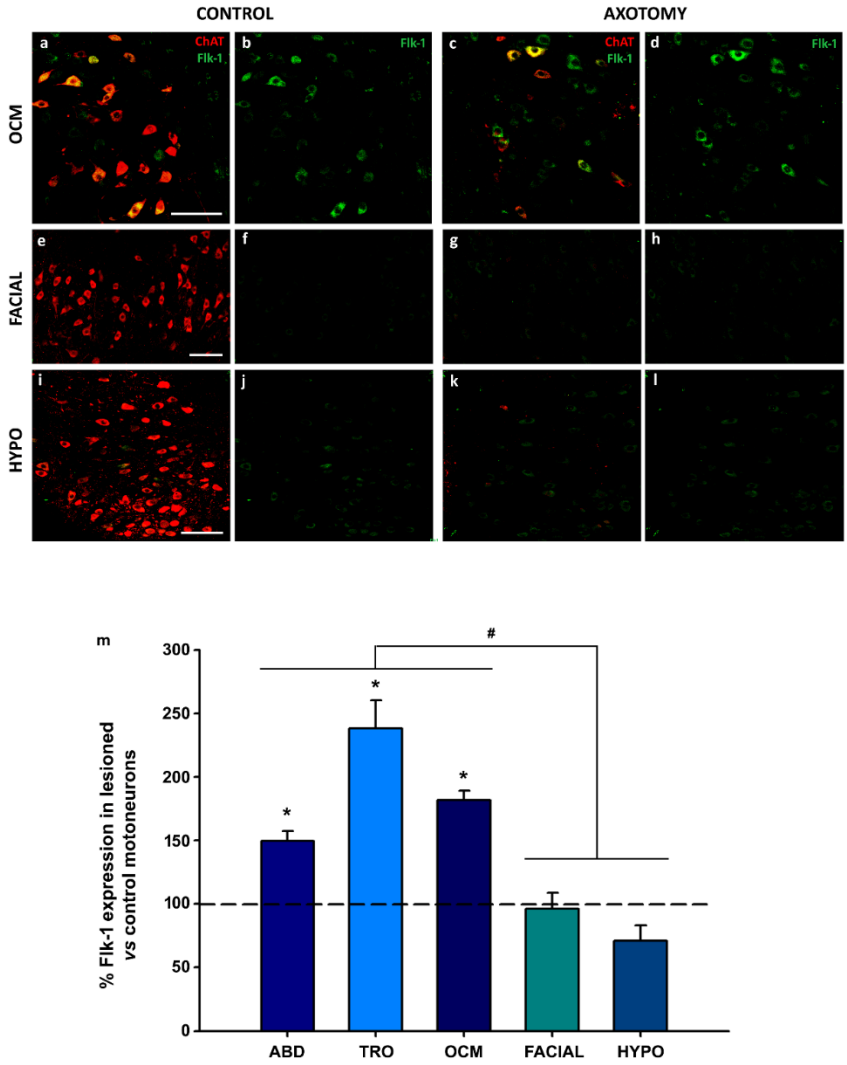

Fig. 7

Flk-1 immunoreactivity in brainstem motoneurons in response to axotomy. Expression of Flk-1 (in green) increased in motoneurons of the oculomotor system after lesion (c-d) with respect to control ones (a-b). No increase was observed in either the facial (g-h) or hypoglossal motoneurons on the injured side (k-l) compared to those on the control side (e-f and i-j, respectively). Scale bars = 100 μm (in a for a-b; in c for c-d; in e for e-f; in g for g-h; in i for i-j; in k for k-l). Motoneurons were identified by ChAT antibody (in red). (m) The histogram shows the increase of Flk-1 VEGF labelling in the lesioned motoneurons compared to control motoneurons (= 100 %) (*: paired t-test; $p < 0.05$; n = 4 animals) of the oculomotor system, but no differences were obtained between control and injured motoneurons of the facial and hypoglossal nuclei. When the increase of Flk-1 in response to injury was compared between motoneurons of the different nuclei, significant differences were observed between oculomotor and not oculomotor neurons (#: one-way ANOVA test; $p < 0.001$; n = 4 animals).

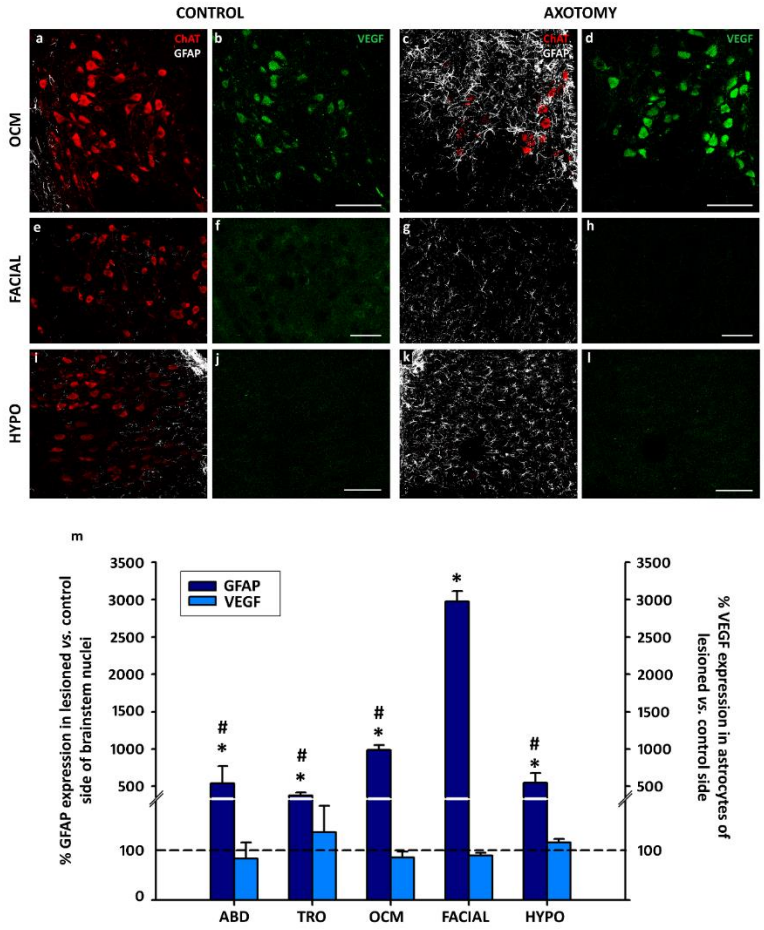

Fig. 8

VEGF immunoreactivity in astrocytes of the brainstem motor nuclei in response to axotomy. Expression of VEGF (in green) in astrocytes (in white) was low in the studied motor nuclei, even after lesion. The confocal images show the expression of VEGF in control OCM nucleus (a-b), and the glial reaction seven days after axotomy (c), producing no increase in VEGF immunolabelling in the reactive astrocytes (c-d). No increase in VEGF was observed either in the astrocytes located in lesioned facial (g-h) and hypoglossal nuclei (k-l), compared to control side (e-f and i-j, respectively). Scale bars = 100 μm (in b for a-b; in d for c-d; in f for e-f; in h for g-h; in j for i-j; in l for k-l). (m) Quantification of GFAP expression in the lesioned nuclei showed a significant increase in all the nuclei (*: paired t-tests; $p < 0.05$; n = 4 animals). That glial reaction was significantly higher in facial nucleus compared to the rest of the nuclei (#: significant differences to facial nuclei; one-way ANOVA test; $p < 0.05$; n = 4 animals). However, VEGF expression did not increase in astrocytes of any cranial motor nuclei after axotomy. No significant differences were observed when the percentage of VEGF in astrocytes of the lesioned sides with respect to their control sides were compared between nuclei (one-way ANOVA test; $p > 0.05$; n = 4 animals).

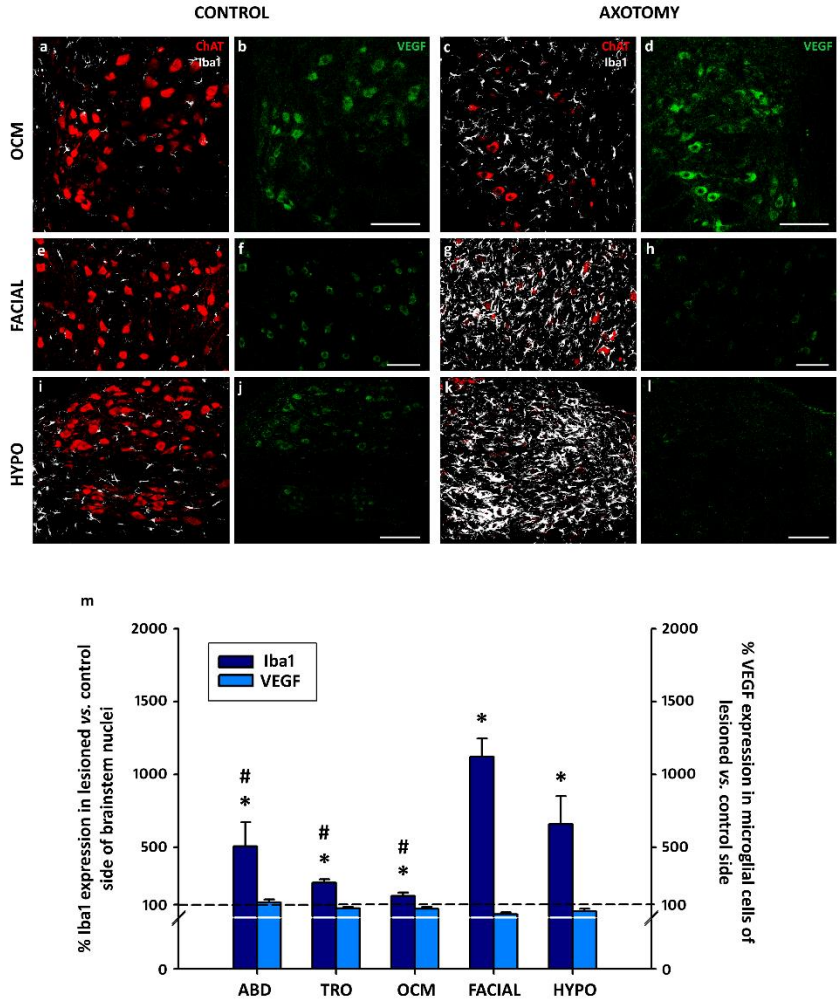

Fig. 9

VEGF immunoreactivity in microglial cells of the brainstem motor nuclei in response to axotomy. Expression of VEGF (in green) in microglial cells (in white) located in the studied motor nuclei was low in all of them, even after lesion. The confocal images show the expression of VEGF in control OCM nucleus (a-b), and the microglial reaction seven days after axotomy (c), producing no increase in vegf immunolabelling in the reactive microglial cells (c-d). There was also no increase in VEGF in the microglial cells located in lesioned facial (g-h) and hypoglossal nuclei (k-l), compared to control side (e-f and i-j, respectively). Scale bars = 100 μm (in b for a-b; in d for c-d; in f for e-f; in h for g-h; in j for i-j; in l for k-l). (m) Quantification of Iba1 expression in the lesioned nuclei showed a significant increase in all the nuclei compared to the respective control nuclei (*: paired t-tests; $p < 0.05$; $n = 4$ animals). That microglial reaction was significantly higher in facial nucleus compared to the ocular motor nuclei (#: significant differences to facial nuclei; one-way ANOVA test; $p < 0.05$; $n = 4$ animals). However, VEGF expression did not increase in microglial cells of cranial motor nuclei after axotomy. No significant differences were observed when the percentage of VEGF in microglial cells of the lesioned sides with respect to their control sides were compared between nuclei (one-way ANOVA test; $p > 0.05$; $n = 4$ animals).

	Control	Axotomy
Ocular motoneurons	++	+++
Facial motoneurons	+	+
Hypogglosal motoneurons	+	+
Astrocytes	+	+
Microglial cells	+	+
Extraocular muscles	+	
Buccinator muscle	+	
Tongue muscles	+	

Table 1

Intensity of VEGF signals in the cytoplasm of diverse cell types located in brainstem motor nuclei in control situation and after axotomy. +: low intensity; ++: high intensity; +++: very high intensity.